

Boltzmann Neutrino Transport Simulation of Core-collapse Supernovae and Collective Neutrino Oscillation

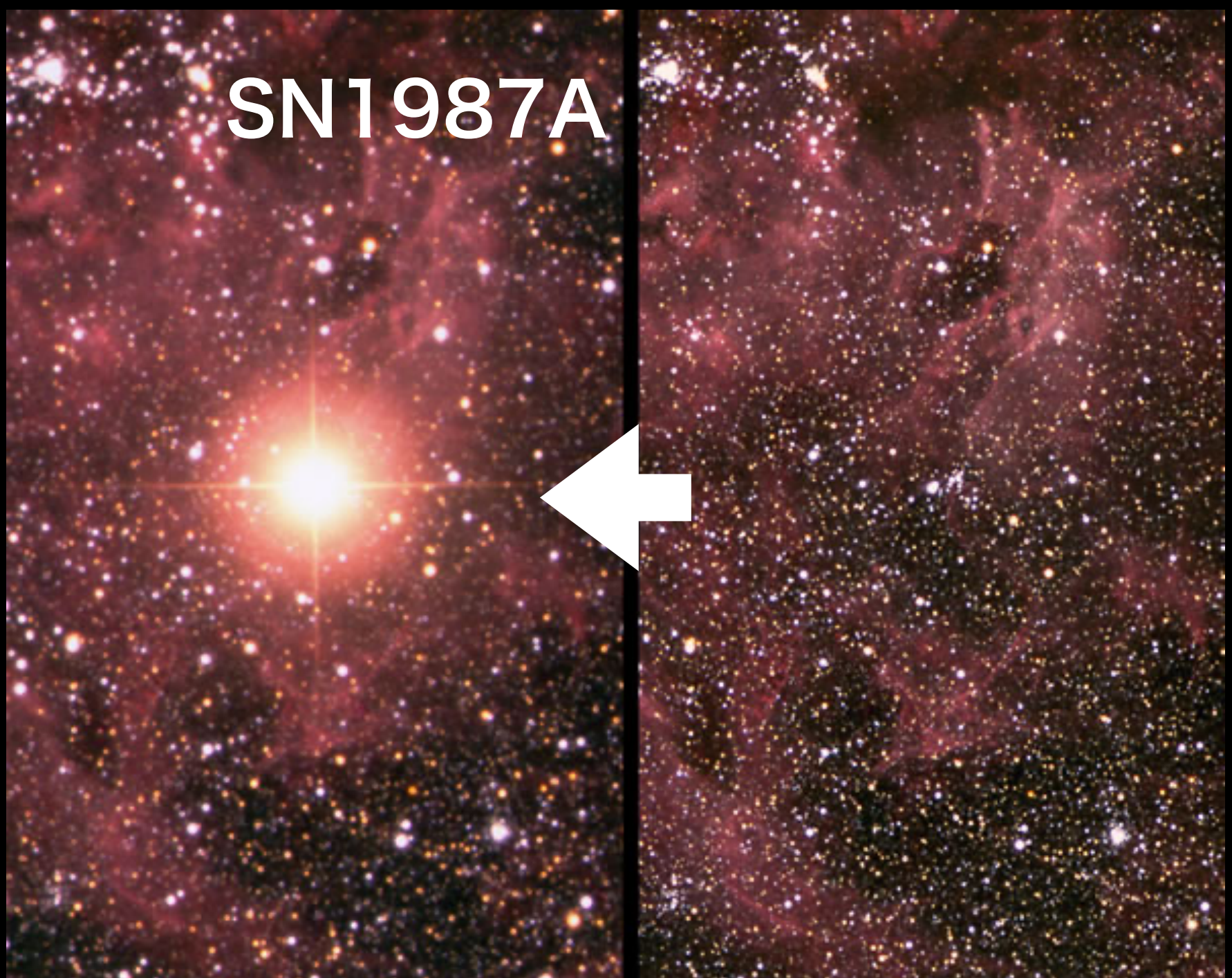
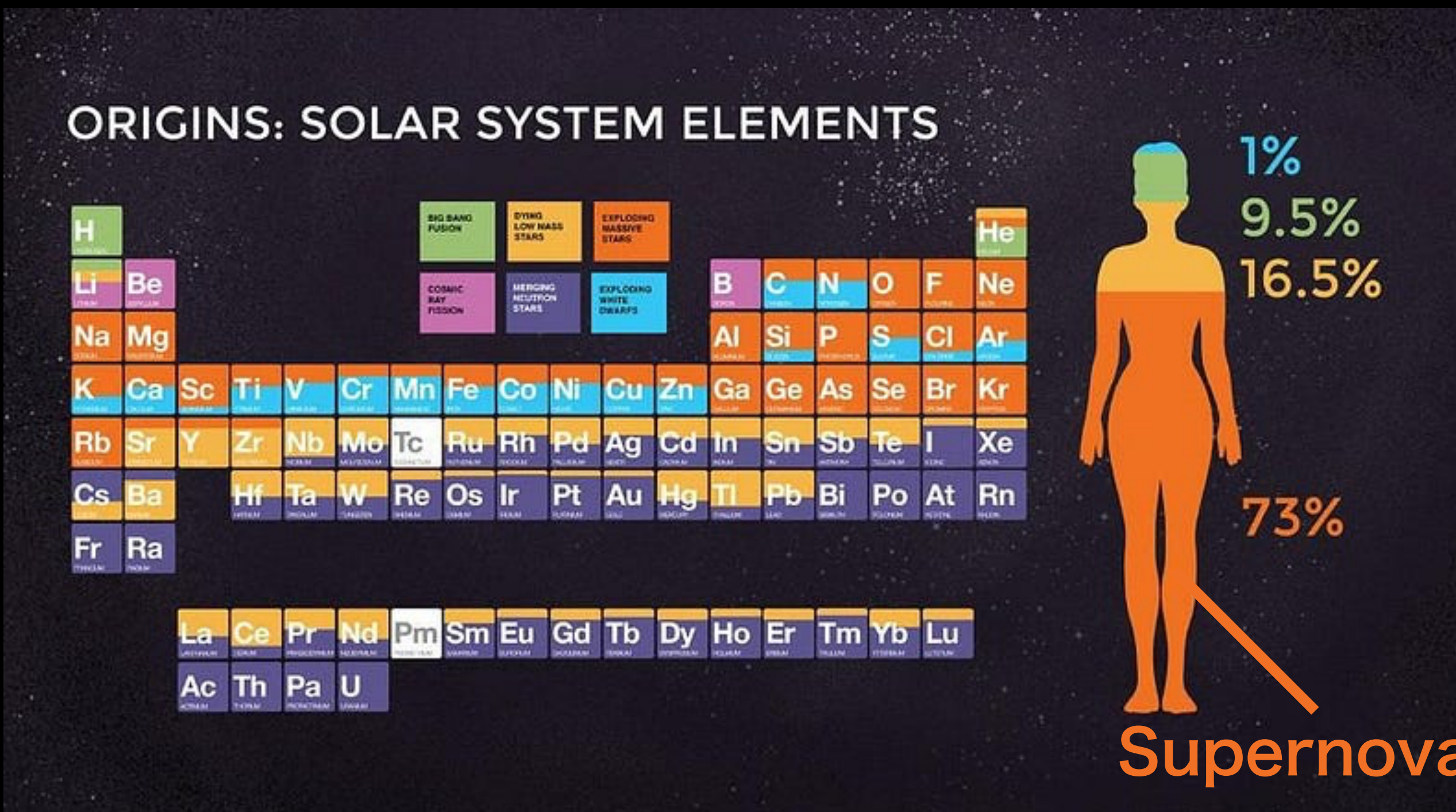
Based on

- R. Akaho et al, PRD 109, 023012 (2024)
- J. Liu, R. A. et al, PRD 108, 123024 (2023)
- J. Liu, H.Nagakura, R. A. et al, arXiv:2407.10604
- R. A. et al, in prep.

Ryuichiro Akaho
(Waseda University)

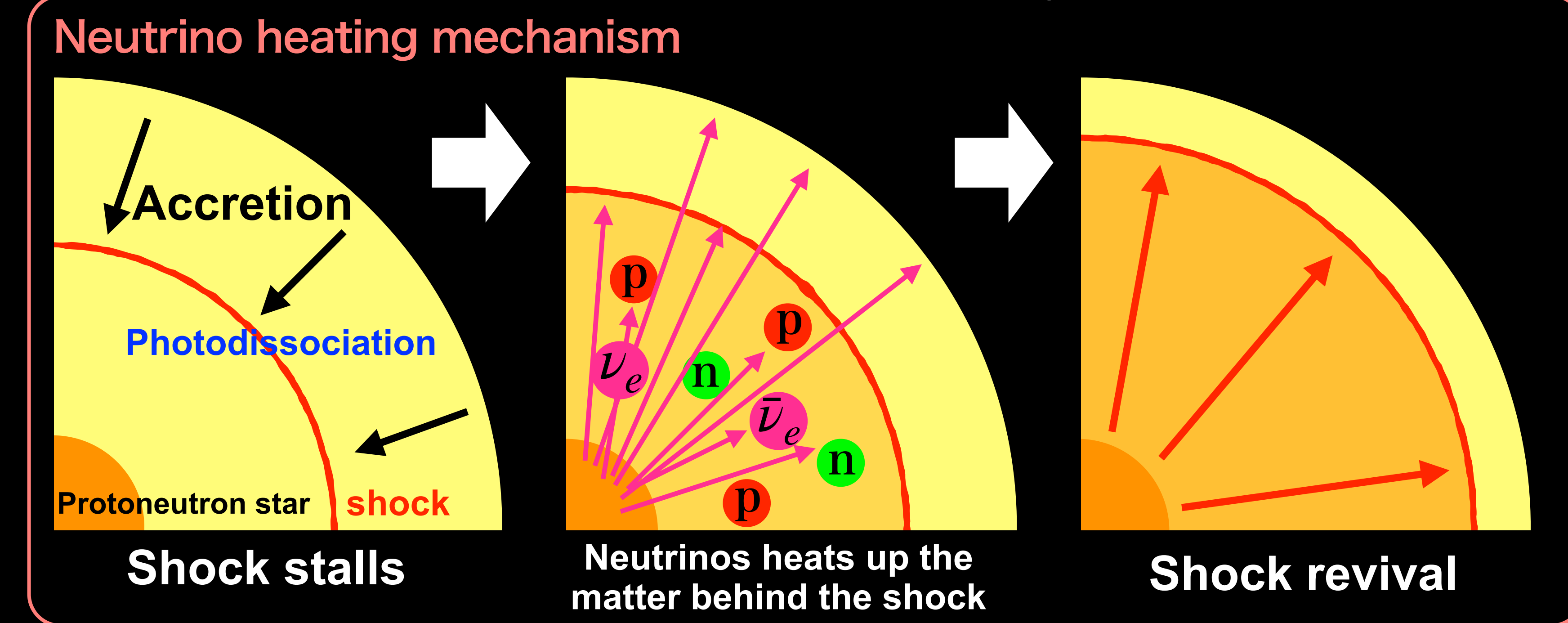
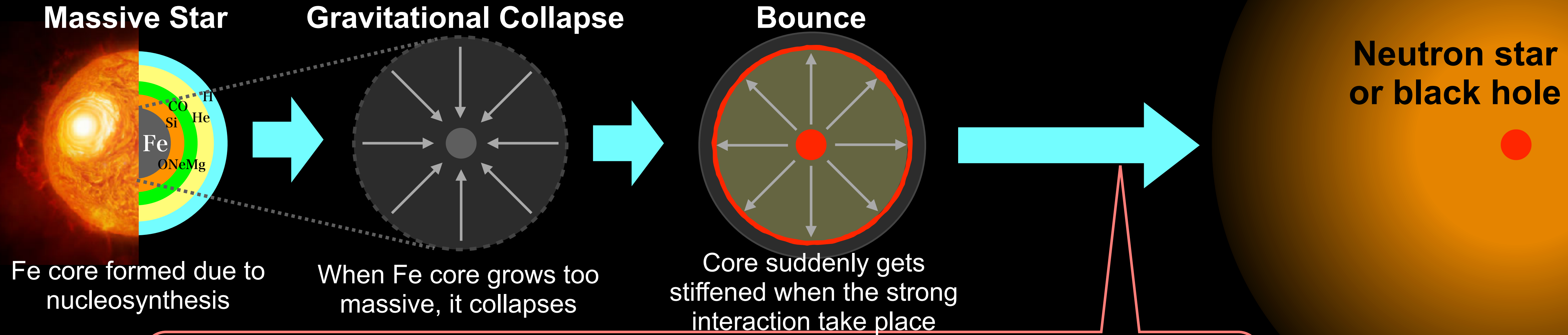
Core-collapse Supernovae (CCSNe)

- Energetic explosion occurring at the end of stellar evolution.
- It synthesizes various elements in our universe,



Scenario of CCSN

Explosion



Aim of CCSN Simulation

Reproducing Existing Observations

- Reproduce explosion energy, synthesized ^{56}Ni mass inferred from electromagnetic observation
- Current state-of-the-art simulation still cannot reproduce observed values

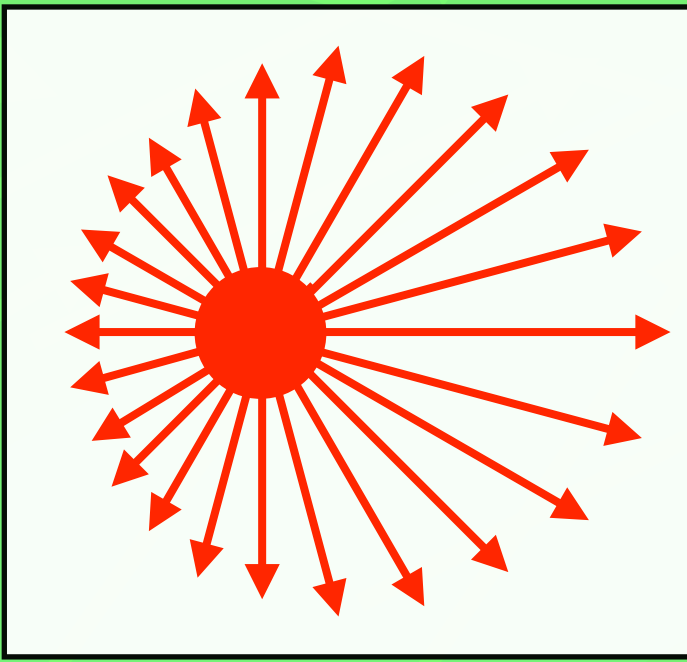
Construct Theoretical Model for Future Observations

- Accurate theoretical model should be prepared in preparation for future observations.
- Unfortunately, there are still large uncertainties remaining due to numerical methods.

Neutrinos inside CCSN

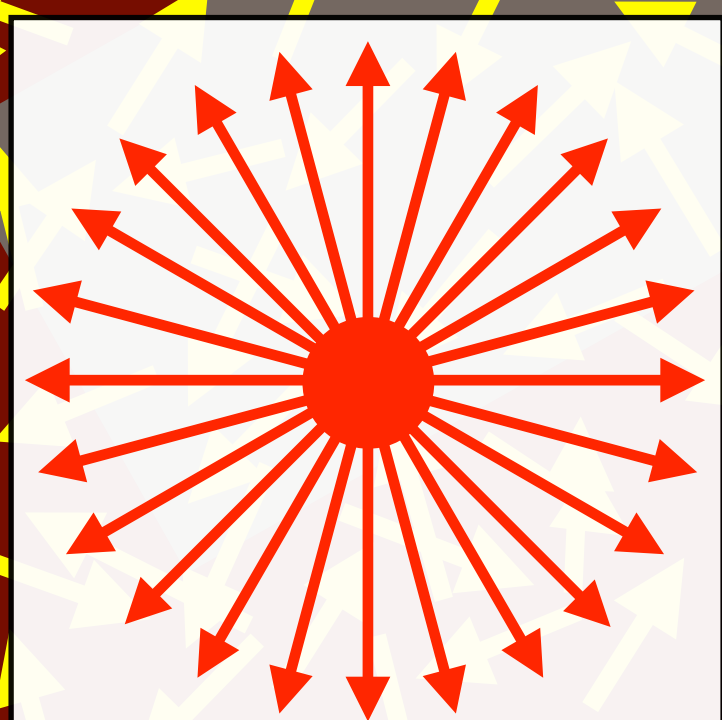
Free streaming

Intermediate: nontrivial



thermal eq. (Fermi-Dirac)

momentum: isotropic



Phase space distribution function $f(x^\mu, p^i)$

Boltzmann equation

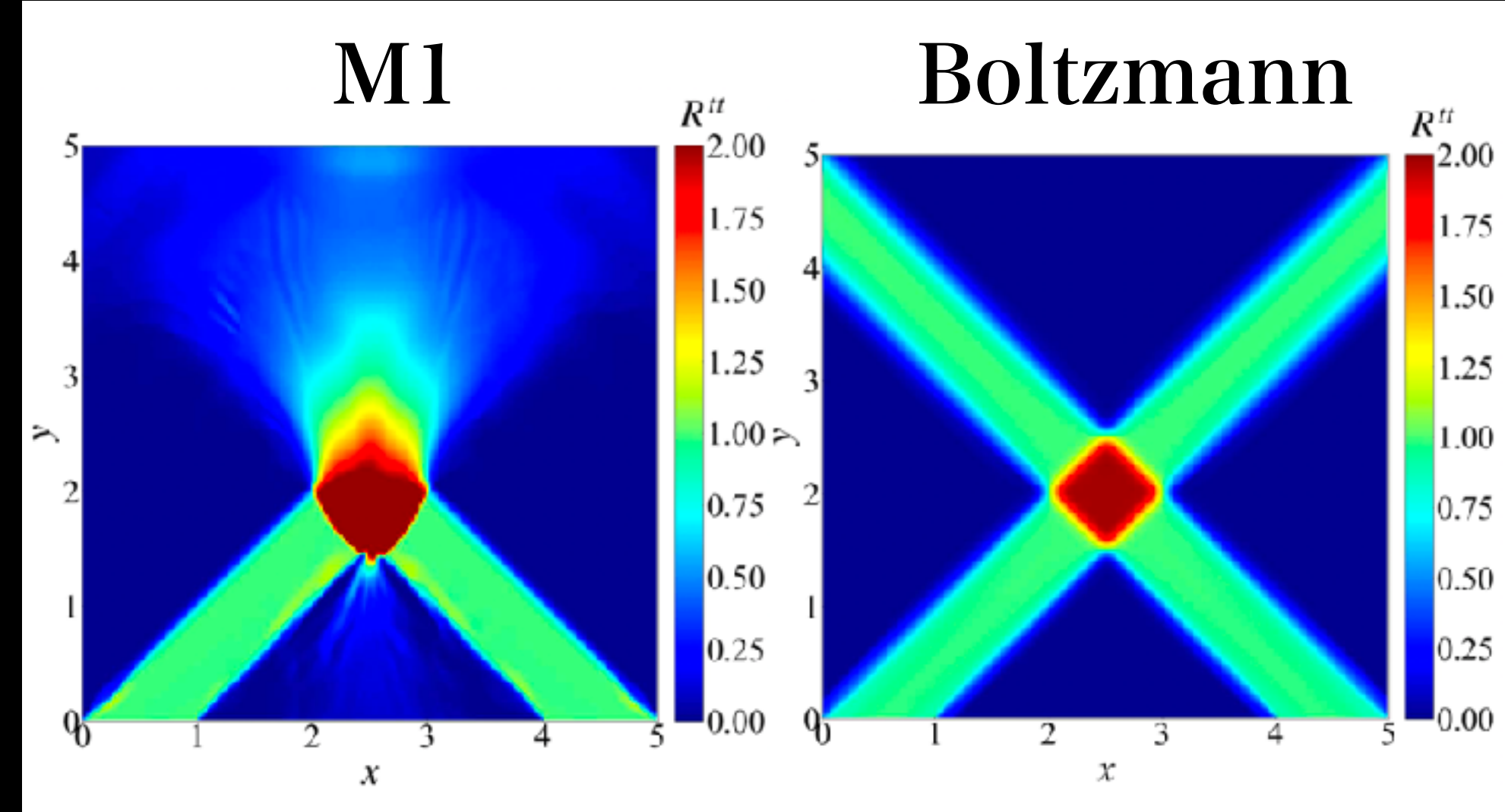
$$p^\alpha \frac{\partial f}{\partial x^\alpha} - \Gamma_{\alpha\beta}^i p^\alpha p^\beta \frac{\partial f}{\partial p^i} = \left[\frac{\delta f}{\delta t} \right]_{\text{coll}}$$

The equation is shown with three horizontal bars below it: a red bar under the first term, an orange bar under the second term, and a green bar under the bracketed term.

Example of Approximate Transport

Two-moment neutrino transport

Reduce momentum space information in order to save computational cost



Distribution Function

$$f(r, \theta, \phi, \epsilon, \theta_\nu, \phi_\nu)$$

Boltzmann Equation

$$\frac{\partial f}{\partial t} + p^i \frac{\partial f}{\partial x^i} + \dot{p}^i \frac{\partial f}{\partial p^i} = C$$



Multiply angular cosines in the momentum space and integrate

Moments

$$E(r, \theta, \phi, \epsilon) \quad F^i(r, \theta, \phi, \epsilon) \quad P^{ij}(r, \theta, \phi, \epsilon)$$

Moment Equations

$$\frac{\partial E}{\partial t} = L_1(E, F^i, P^{ij}) \quad \frac{\partial F^i}{\partial t} = L_2(E, F^i, P^{ij})$$

$$\text{Closure: } P_{M1}^{ij} = \frac{3\chi - 1}{2} P_{thin}^{ij} + \frac{3(1 - \chi)}{2} P_{thick}^{ij}$$

Boltzmann Neutrino Radiation Hydrodynamics Code

Boltzmann equation wrt phase space distribution function $f(t, t, \theta, \phi, \epsilon, \theta_\nu, \phi_\nu)$

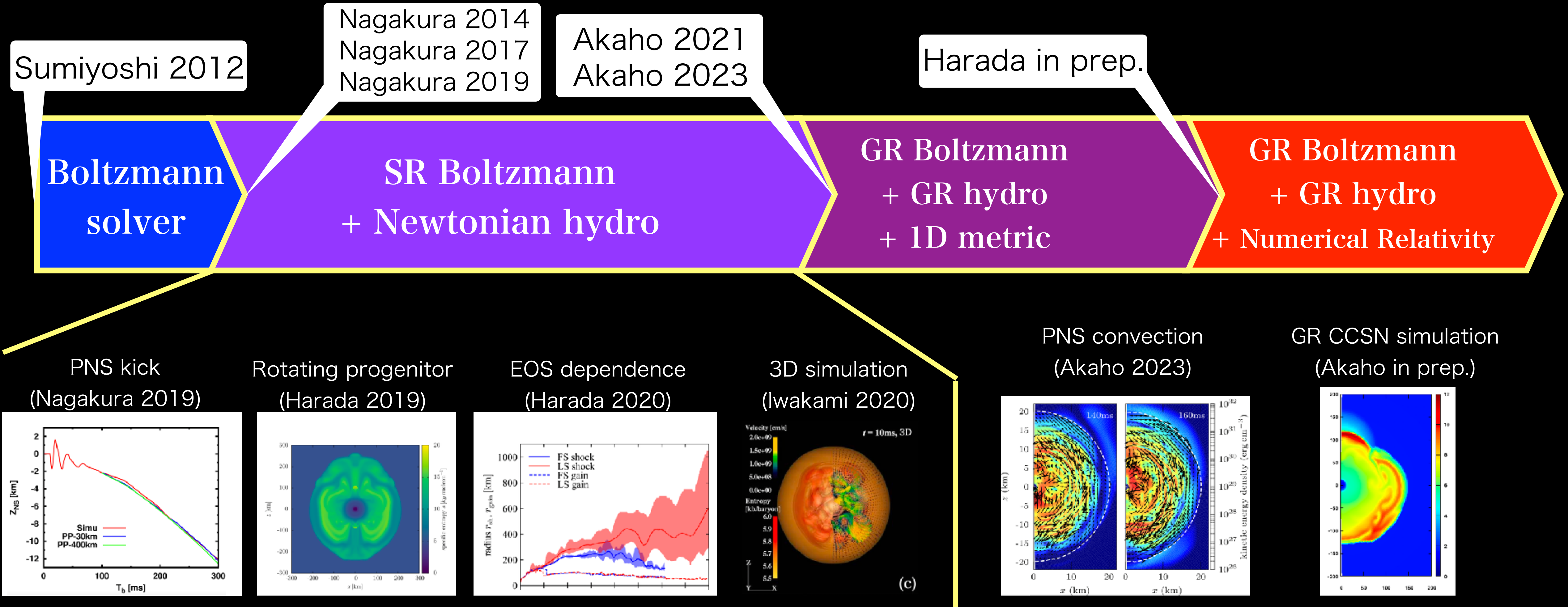
$$\frac{1}{\sqrt{-g}} \frac{\partial}{\partial x^\mu} \left[\left(e_{(0)}^\mu + \sum_{i=1}^3 l_i e_{(i)}^\mu \right) \sqrt{-g} f \right] - \frac{1}{\epsilon^2} \frac{\partial}{\partial \epsilon} \left(\epsilon^3 f \omega_{(0)} \right) + \frac{1}{\sin \theta_\nu} \frac{\partial}{\partial \theta_\nu} \left(\sin \theta_\nu f \omega_{(\theta_\nu)} \right) - \frac{1}{\sin^2 \theta_\nu} \frac{\partial}{\partial \phi_\nu} \left(f \omega_{(\phi_\nu)} \right) = S_{\text{rad}}$$

Spacetime advection (propagation)	Energy advection (grav. red/blue shift)	Angular advection (zenith angle θ_ν)	Angular advection (azimuth angle ϕ_ν)	Collision (ν -matter interaction)
$l_{(1)} = \cos \theta_\nu$	$\omega_{(0)} \equiv \epsilon^{-2} p^\mu p_\nu \nabla_\mu e_{(0)}^\nu$	$\omega_{(i)} \equiv \sum_{i=1}^3 \omega_{(i)} \frac{\partial l_{(i)}}{\partial \theta_\nu}$	$\omega_{(\phi_\nu)} \equiv \sum_{i=2}^3 \omega_{(i)} \frac{\partial l_{(i)}}{\partial \phi_\nu}$	
$l_{(2)} = \sin \theta_\nu \cos \phi_\nu$	$\omega_i \equiv \epsilon^{-2} p^\mu p_\nu \nabla_\mu e_{(i)}^\nu$			
$l_{(3)} = \sin \theta_\nu \sin \phi_\nu$				

Hydrodynamics equation

Continuity eq.	$\partial_t \rho_* + \partial_j (\rho_* v^j) = 0$
Momentum cons.	$\partial_t S_i + \partial_j (S_i v^j + \alpha \sqrt{\gamma} P \delta_i^j) = - S_0 \partial_i \alpha + S_j \partial_i \beta^j - \frac{1}{2} \alpha \sqrt{\gamma} S_{jk} \partial_i \gamma^{jk} - \alpha \sqrt{\gamma} G_i$
Energy cons.	$\partial_t (S_0 - \rho_*) + \partial_k ((S_0 - \rho_*) v^k + \sqrt{\gamma} P (v^k + \beta^k)) = \alpha \sqrt{\gamma} S^{ij} K_{ij} - S_i D^i \alpha + \alpha \sqrt{\gamma} n^\mu G_\mu$
Lepton num. cons.	$\partial_t (\rho_* Y_e) + \partial_j (\rho_* Y_e v^j) = - \alpha \sqrt{\gamma} \Gamma$
$\rho_* = \alpha \sqrt{\gamma} \rho_0 u^t = \sqrt{\gamma} \rho_0 \omega$ $S_0 = \sqrt{\gamma} (\rho h w^2 - P)$ $S_j = \rho_* h u_j$ $S_{ij} = \rho h u_i u_j + P \gamma_{ij}$	

Boltzmann Radiation-hydro Simulation



Basics of Neutrino Oscillation

Liouville von Neumann Eq.

$$\rho \equiv \begin{pmatrix} f_{\nu_e} & S_{ex} \\ S_{xe} & f_{\nu_x} \end{pmatrix}$$

Diagonal components correspond to neutrino density

$$iv^\mu \partial_\mu \rho = \left[\frac{m_1^2 + m_2^2}{4E} \begin{pmatrix} 1 & 0 \\ 0 & 1 \end{pmatrix} + \frac{m_2^2 - m_1^2}{4E} \begin{pmatrix} -\cos 2\theta_{12} & \sin 2\theta_{12} \\ \sin 2\theta_{12} & \cos 2\theta_{12} \end{pmatrix} + \sqrt{2} G_F n_e \begin{pmatrix} 1 & 0 \\ 0 & 0 \end{pmatrix}, \rho \right]$$

Vacuum (mass difference leads to oscillation)

Matter (only diagonal)

neutrino oscillation has been neglected for CCSN core

Dilute matter ($\rho \ll 10^5 \text{ g/cc}$): vacuum oscillation

Vacuum potential = matter potential: MSW resonance

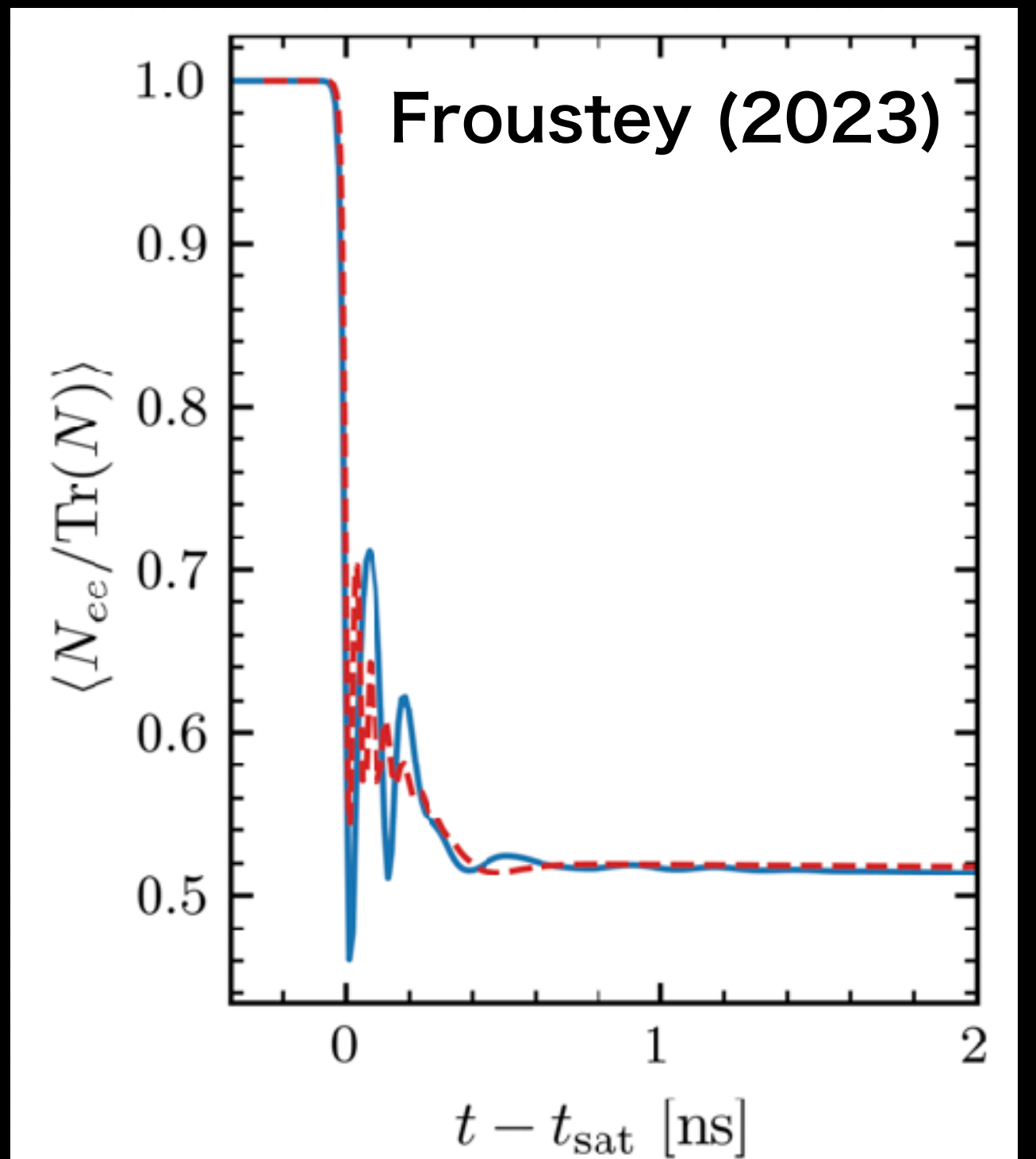
High density matter ($\rho \gg 10^5 \text{ g/cc}$): matter suppression (no oscillation)

Collective Neutrino Oscillation

$$iv^\mu \partial_\mu \rho = \left[H_{\text{vac}} + H_{\text{mat}} + \sqrt{2} G_F v_\mu \int dP' \rho(x, P') v'^\mu, \rho \right]$$

neutrino self-interaction

- Inside CCSNe or neutron star mergers, "collective oscillation" may occur due to high neutrino density
- It can dramatically change neutrino distribution, which may affect CCSN dynamics/signals, and also BNSMs.



Timescale

Collective	Weak interaction	Dynamical
$t_{\nu\nu} \sim \frac{1}{cG_F n_\nu} \sim 10^{-9} \text{ sec}$	$<$	$t_{\text{weak}} \sim \frac{m_u}{cG_F E_\nu^2 \rho} \sim 10^{-8} \text{ sec}$

Collective Neutrino Flavor Instabilities

$$iv^\mu \partial_\mu \rho = \left[\underline{H_{\text{vacuum}}} + \underline{H_{\text{matter}}} + H_{\nu\nu}, \rho \right] + iC$$

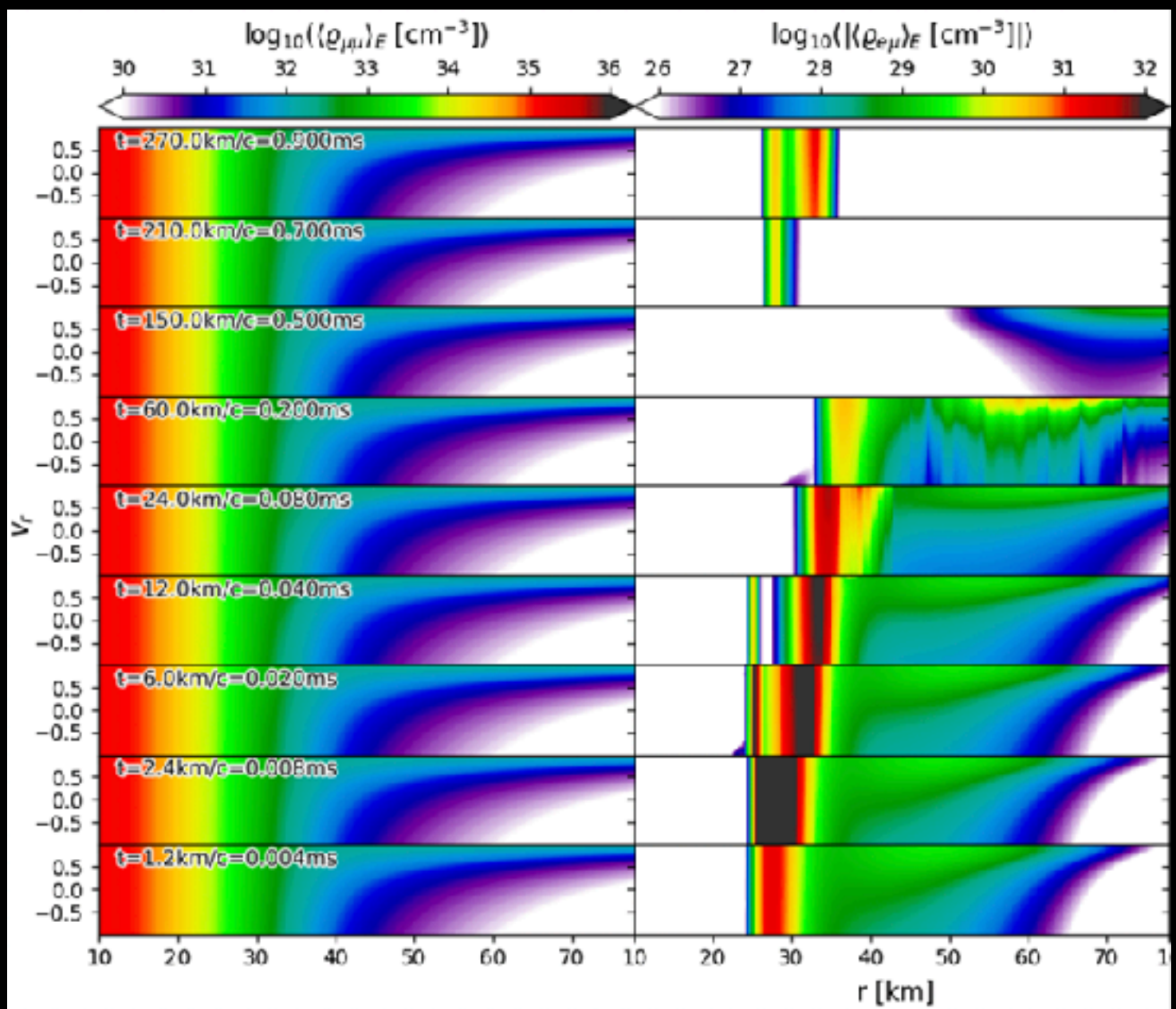
- **Slow instability**
Energy crossing
- **Fast instability**
Angular crossing in momentum space
Requires multi-angle neutrino transport
- **Collisional instability**
Disparity in collision rates

Global Simulation of Collective Oscillation

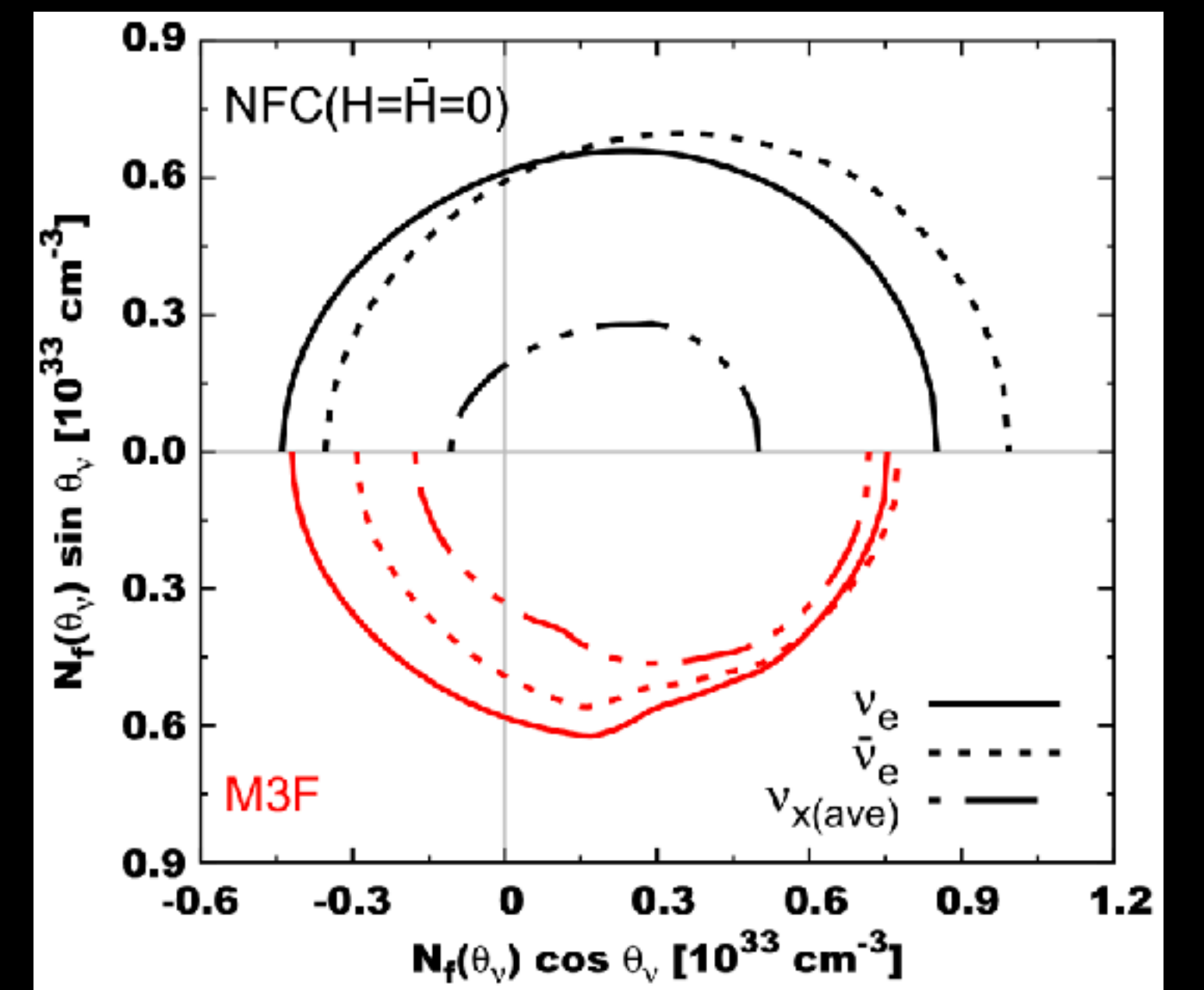
- Ideally, full quantum equation should be solved for the neutrino transport.
- However, it is too computationally expensive (**typical wavelength** $\sim \text{cm}!$)

CCSNe

Xiong 2023

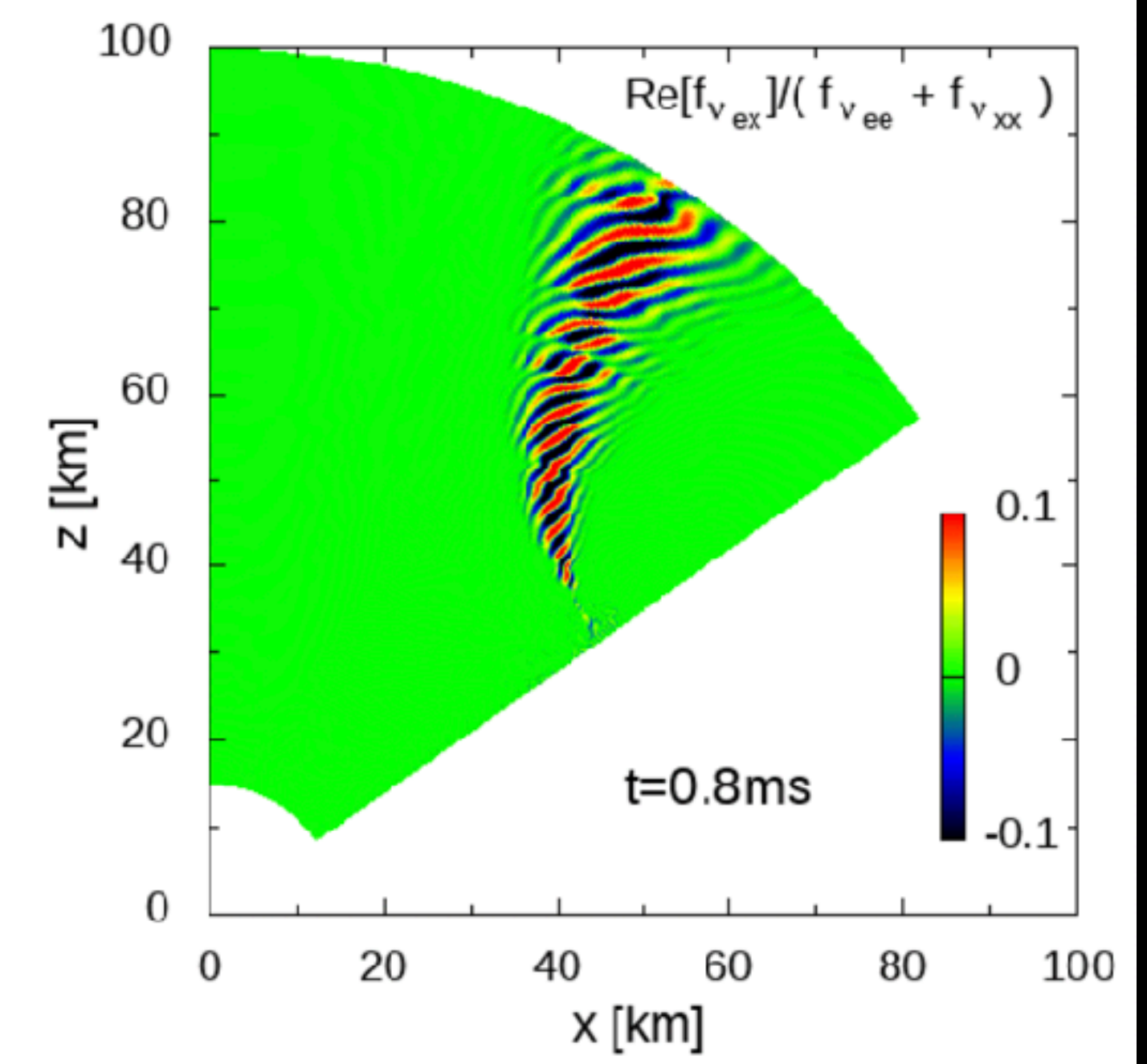


Nagakura 2023



BNMSSs

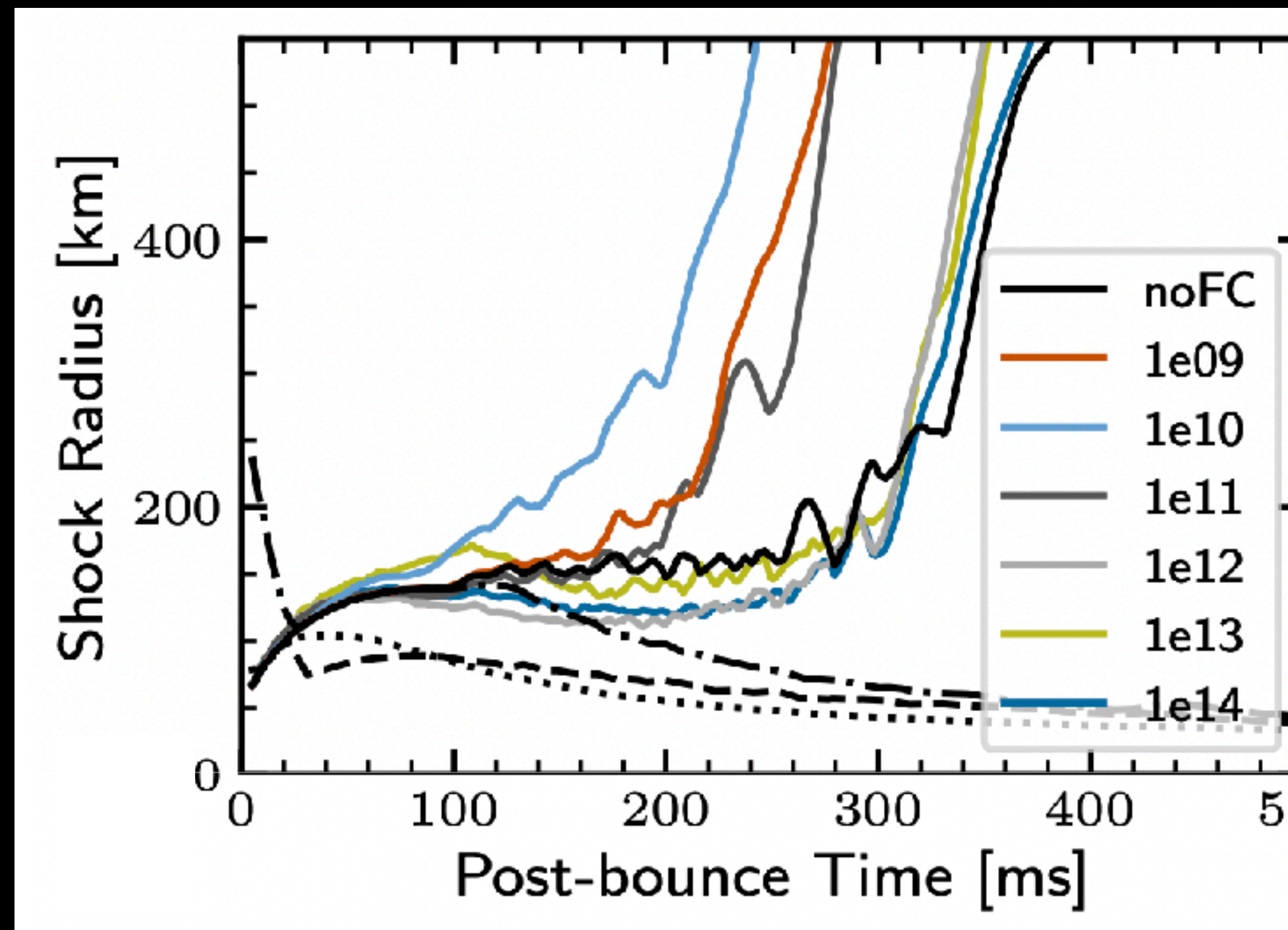
Nagakura 2023



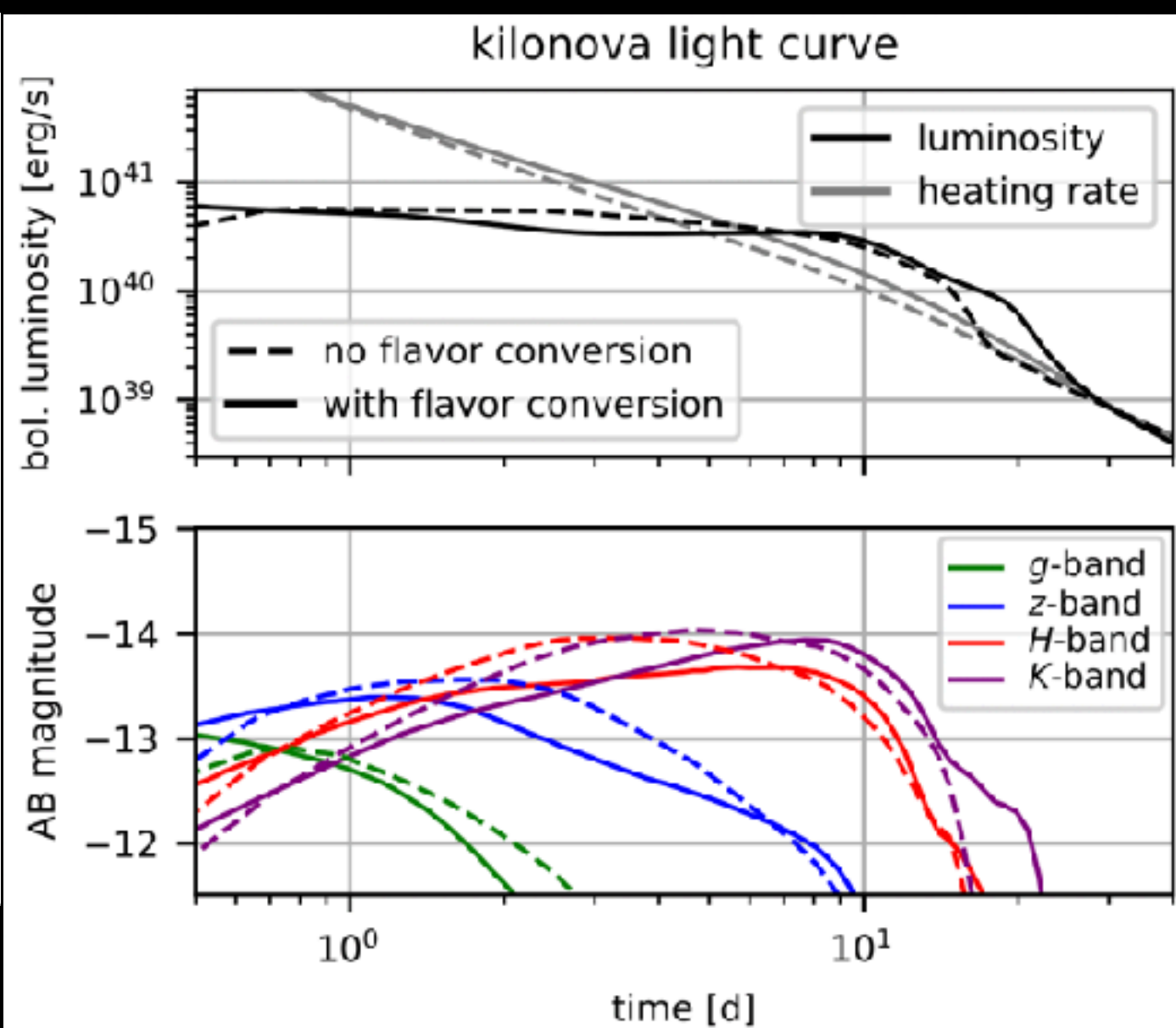
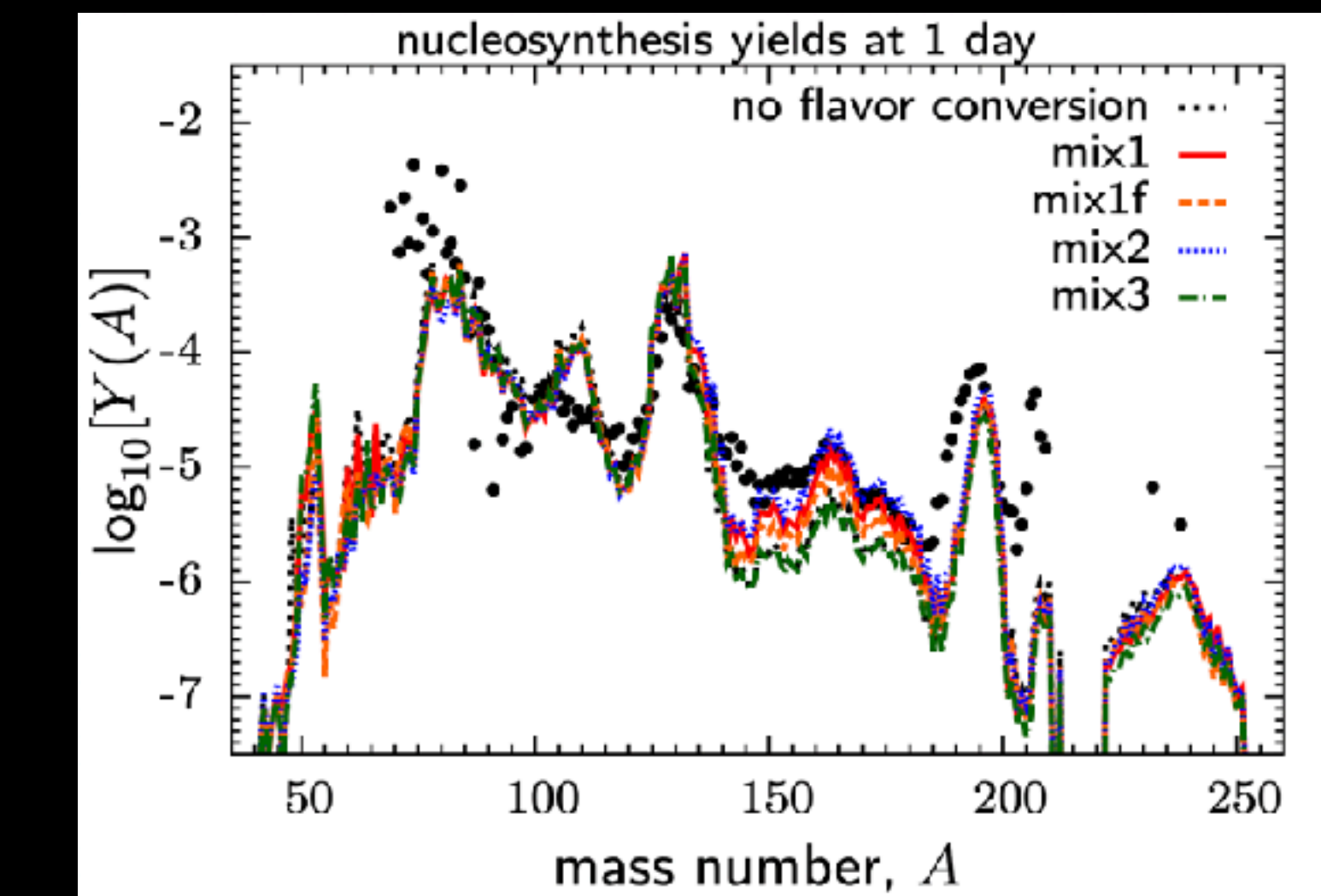
Classical Simulation + Mixing

- There are several attempts to include the effects of flavor conversion to the classical simulations.
- However, (1)detecting the flavor instability and (2)imposing neutrino distribution after the flavor conversion is tighly nontrivial problem.

CCSN simulation with flavor mixing
Ehring 2023



BH accretion disk simulation
with flavor mixing

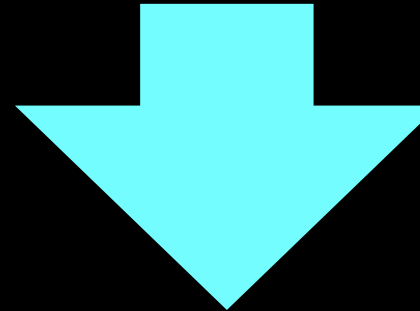


Just 2022

Linear Stability Analysis

In this study, linear stability analysis (LSA) is performed to judge the occurrence of collective oscillation

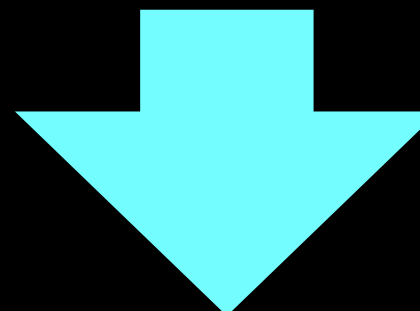
$$iv^\mu \partial_\mu \rho = \left[\sqrt{2} G_F v^\mu \int dP' \rho(x, P') v'_\mu, \rho \right] + \frac{i}{2} \{ \text{diag}(\Gamma_{\nu_e}(x, P), \Gamma_{\nu_x}(x, P)), \rho_{\text{eq}} - \rho \}$$



Assuming $f \gg S$, the off-diagonal component becomes

$$v^\mu (i\partial_\mu - \Lambda_{0e\mu} + \Lambda_{0x\mu}) S_{ex} + i\Gamma_{ex} S_{ex} = 0$$

$$\Lambda_{0\alpha}^\mu \equiv \int dP f_{\nu_\alpha}(x, P) v^\mu$$



Plane-wave ansatz $S_{ex}(x, P) = \tilde{S}_{ex}(x, k) e^{ikx}$

$$\Pi_{ex}^{\mu\nu}(k) a_\nu(k) = 0$$

$$\Pi_{ex}^{\mu\nu}(k) = \eta^{\mu\nu} + \sqrt{2} G_F \int dP \frac{(f_{\nu_e} - f_{\nu_x}) v^\mu v^\nu}{v^\lambda (k_\lambda - \Lambda_{0e\lambda} + \Lambda_{0x\lambda}) + i\Gamma_{ex}}$$

$$a^\mu(k) \equiv \sqrt{2} G_F \int dP \tilde{S}_{ex}(k, P) v^\mu$$

$$\rho \equiv \begin{pmatrix} f_{\nu_e} & S_{ex} \\ S_{xe} & f_{\nu_x} \end{pmatrix}$$

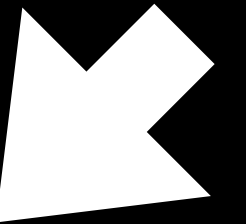
$$\Pi_{ex}^{\mu\nu}(k)a_\nu(k) = 0$$

For the existence of nontrivial solution of a , $\det \Pi_{ex}(k) = 0$ **Dispersion relation**

If ω has **negative imaginary part**, off-diagonal component **grows exponentially** with time.

In this study, two limits are considered to analytically estimate the growth rate.

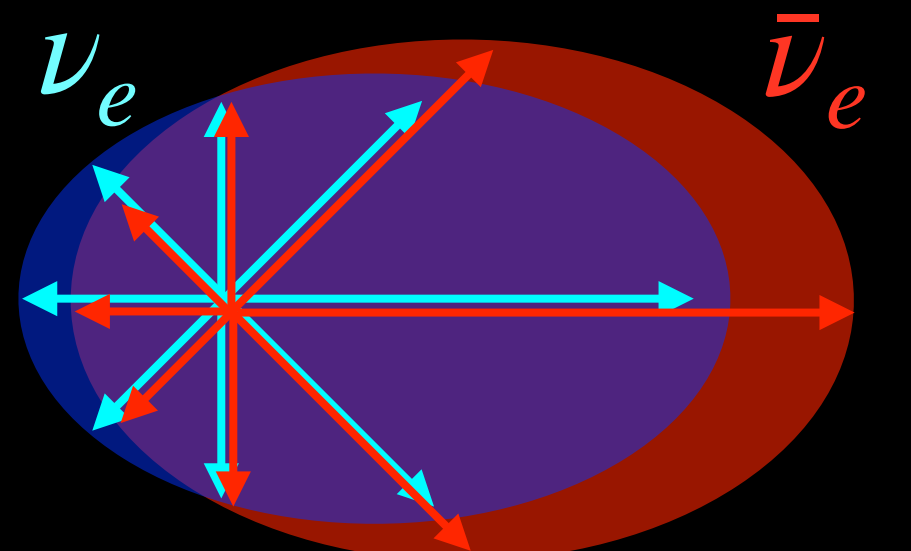
Neglect collision terms



Neglect angular distribution

Fast Flavor Instability (FFI)

- Equivalent to the angular crossing (Morinaga 2021)
(requires Boltzmann neutrino transport!)
- Growth rate proportional to ν density



Collisional Flavor Instability (CFI)

- Caused by the existence of collision terms
- Growth rate proportional to the square-root of neutrino density.

(Most of previous studies only consider FFI)

Growth Rate (FFI)

For a two-beam model, the growth rate is given as

$$\sigma = (1 - \nu_{\nu_e} \cdot \nu_{\bar{\nu}_e}) \operatorname{Re} \sqrt{-F_{\nu_e} F_{\bar{\nu}_e}}$$



with the collimated beams

$$4\pi F_{\bar{\nu}_e} \delta(\nu - \nu_{\bar{\nu}_e}) \quad 4\pi F_{\nu_e} \delta(\nu - \nu_{\nu_e})$$

Above suggests following formula to estimate the growth rate for arbitrary distribution

$$\sigma \equiv \sqrt{-\left(\int_{\Delta G > 0} \frac{d\Omega}{4\pi} \Delta G \right) \left(\int_{\Delta G < 0} \frac{d\Omega}{4\pi} \Delta G \right)}$$
$$\Delta G = \frac{\sqrt{2} G_F}{2\pi^2} \int (f_{\nu_e} - f_{\bar{\nu}_e}) \nu^2 d\nu$$

Growth Rate (CFI)

$$\Pi_{ex}^{\mu\nu}(k) = \eta^{\mu\nu} + \sqrt{2}G_F \int_{-\infty}^{\infty} \frac{E^2 dE}{2\pi^2} \int \frac{d\Omega_p}{4\pi} \frac{f_{\nu_e}(E, v) - f_{\bar{\nu}_x}(E, v)}{\omega - v^\mu k_\mu + i\Gamma_{ex}(E)}$$

1	$\cos\theta_\nu$	$\sin\theta_\nu\cos\phi_\nu$	$\sin\theta_\nu\sin\phi_\nu$
$\cos\theta_\nu$	$\cos^2\theta_\nu$	$\sin\theta_\nu\cos\theta_\nu\cos\phi_\nu$	$\sin\theta_\nu\cos\theta_\nu\sin\phi_\nu$
$\sin\theta_\nu\cos\phi_\nu$	$\sin\theta_\nu\cos\theta_\nu\cos\phi_\nu$	$\sin^2\theta_\nu\cos^2\phi_\nu$	$\sin^2\theta_\nu\cos\phi_\nu\cos\phi_\nu$
$\sin\theta_\nu\sin\phi_\nu$	$\sin\theta_\nu\cos\theta_\nu\sin\phi_\nu$	$\sin^2\theta_\nu\sin\phi_\nu\cos\phi_\nu$	$\sin^2\theta_\nu\sin^2\phi_\nu$

Angular integration is simplified and

nonzero after
integration

$$I \equiv \sqrt{2}G_F \int_{-\infty}^{\infty} \frac{E^2 dE}{2\pi^2} \frac{f_{\nu_e}(E) - f_{\bar{\nu}_x}(E)}{\omega + i\Gamma_{ex}(E)} = -1,3$$

By imposing a monochromatic distribution,

$$\sigma \equiv \text{Im}\omega$$

Isotropy-preserving branch ($I = -1$)

$$\omega_{\pm}^{\text{pres}} = -A - i\gamma \pm \sqrt{A^2 - \alpha^2 + 2iG\alpha},$$

Isotropy-breaking branch ($I = 3$)

$$\omega_{\pm}^{\text{break}} = -\frac{A}{3} - i\gamma \pm \sqrt{\left(\frac{A}{3}\right)^2 - \alpha^2 - \frac{2}{3}iG\alpha},$$

$$G \equiv \frac{n_{\nu_e} + n_{\bar{\nu}_e} - n_{\nu_x} - n_{\bar{\nu}_x}}{2}$$

$$A \equiv \frac{n_{\nu_e} - n_{\bar{\nu}_e} - n_{\nu_x} + n_{\bar{\nu}_x}}{2}$$

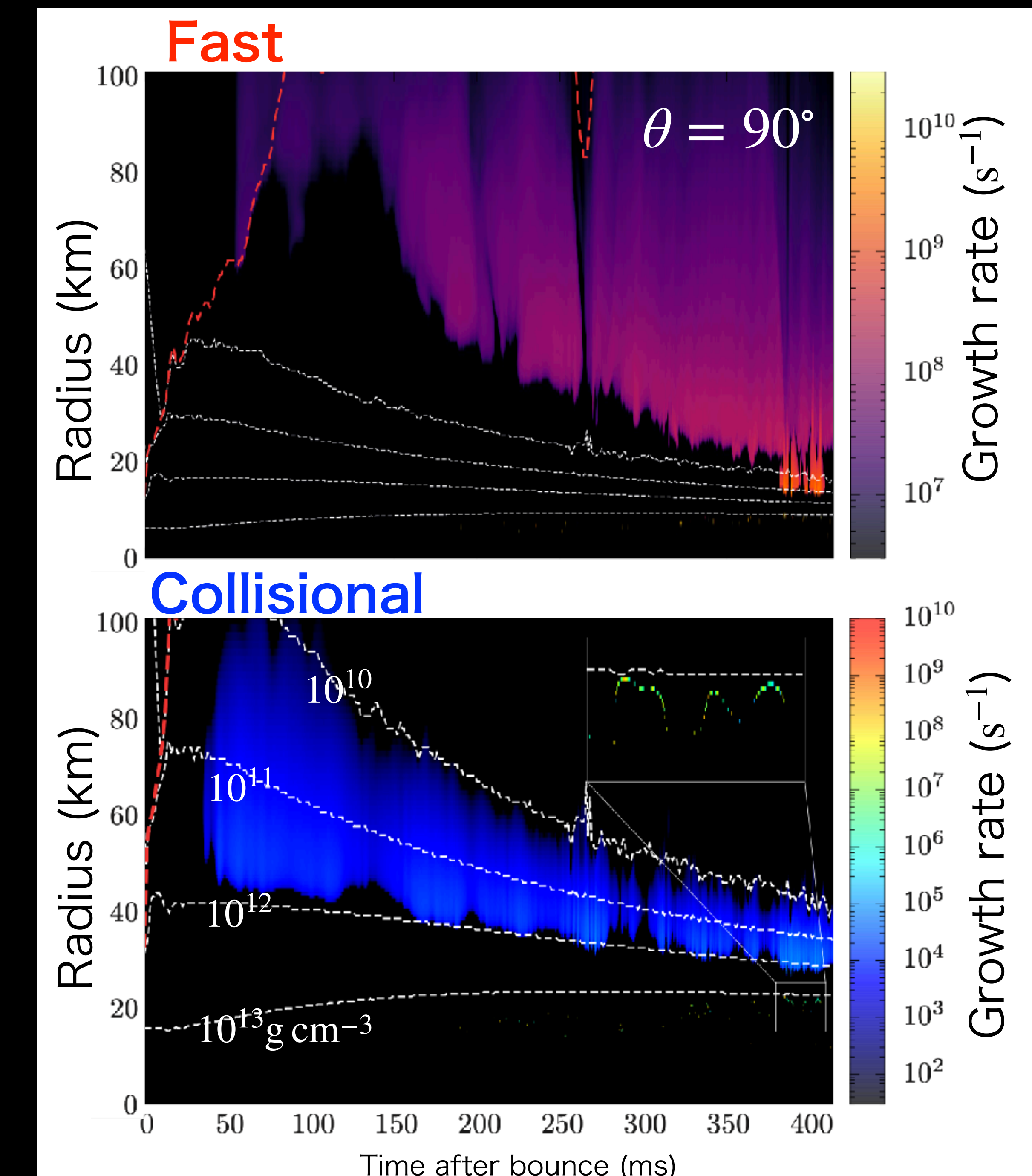
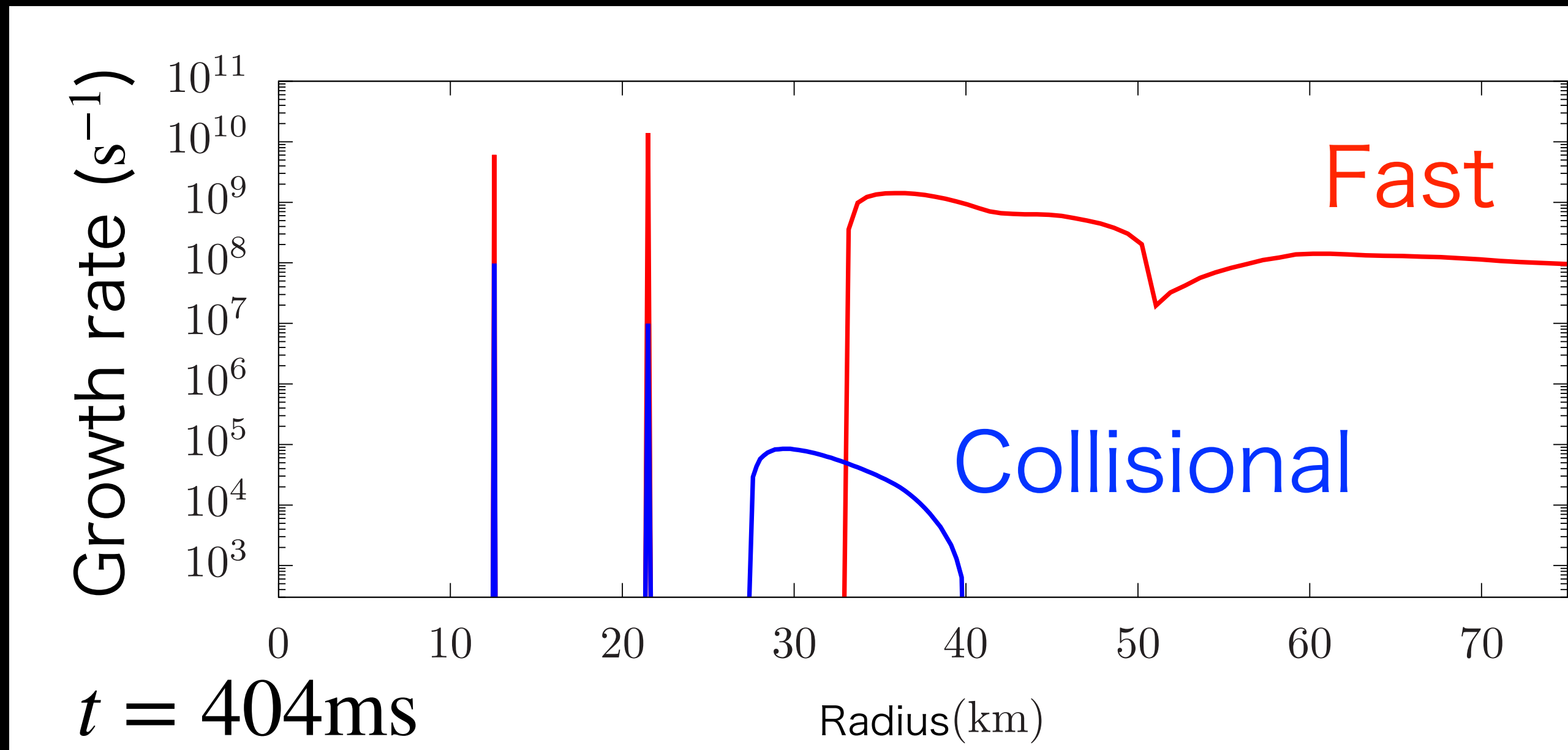
$$\gamma \equiv \frac{\Gamma_{\nu_e} + \Gamma_{\bar{\nu}_e} + \Gamma_{\nu_x} + \Gamma_{\bar{\nu}_x}}{2}$$

$$\alpha \equiv \frac{\Gamma_{\nu_e} - \Gamma_{\bar{\nu}_e} + \Gamma_{\nu_x} - \Gamma_{\bar{\nu}_x}}{2}$$

$$\Gamma_i \equiv \sqrt{2}G_F \int \frac{E^2 dE}{2\pi^2} \Gamma(E)f(E)$$

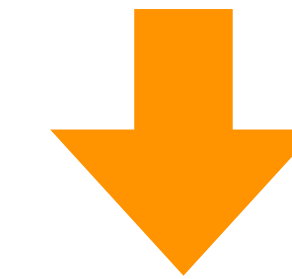
Post-process Analysis

- Stability analysis is performed for 2D CCSN simulation with Boltzmann neutrino transport
- $11.2M_{\odot}$ progenitor, Lattimer-Swesty EOS
- Both CFI and FFI are found, and if both of them occur, FFI dominates

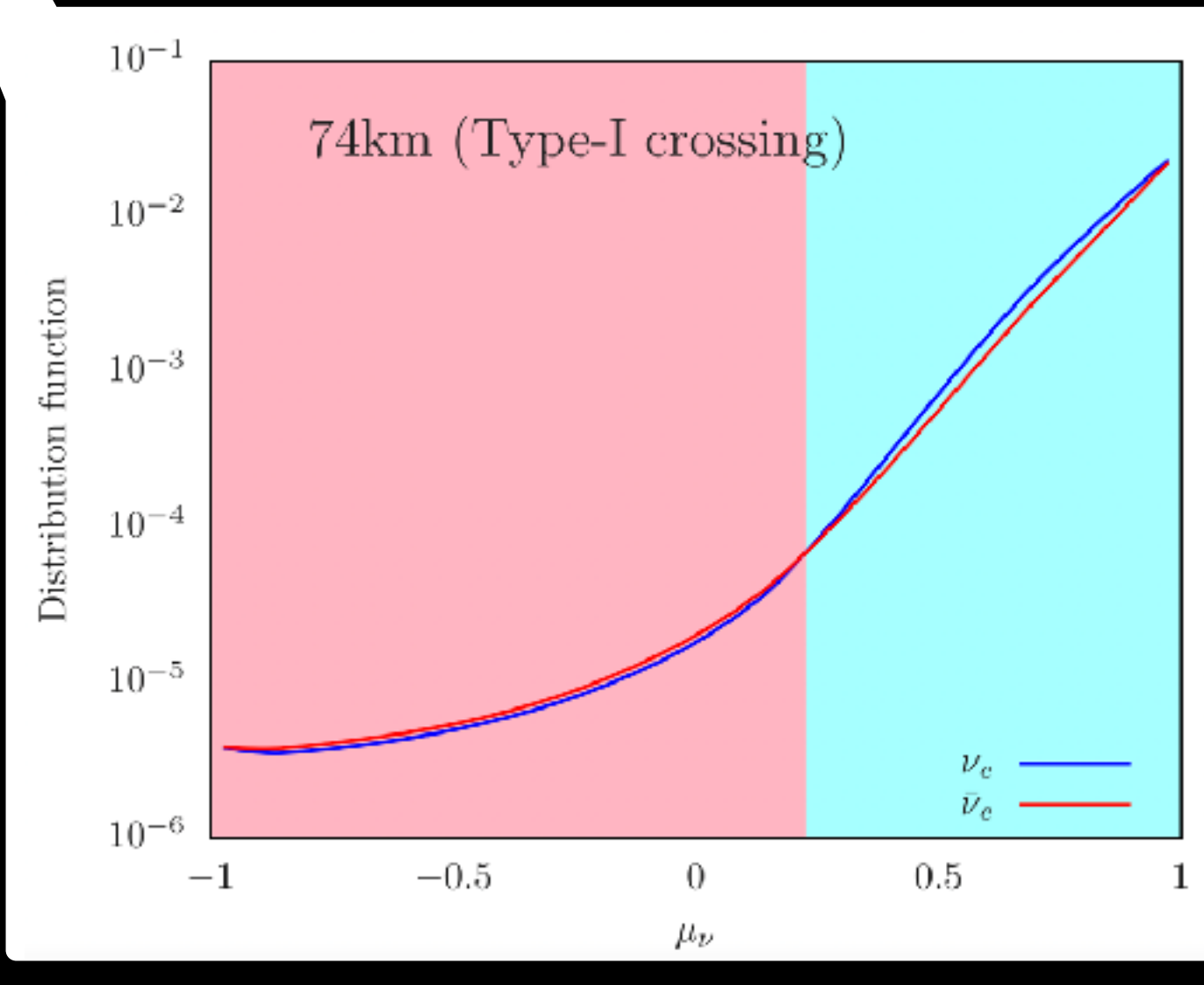
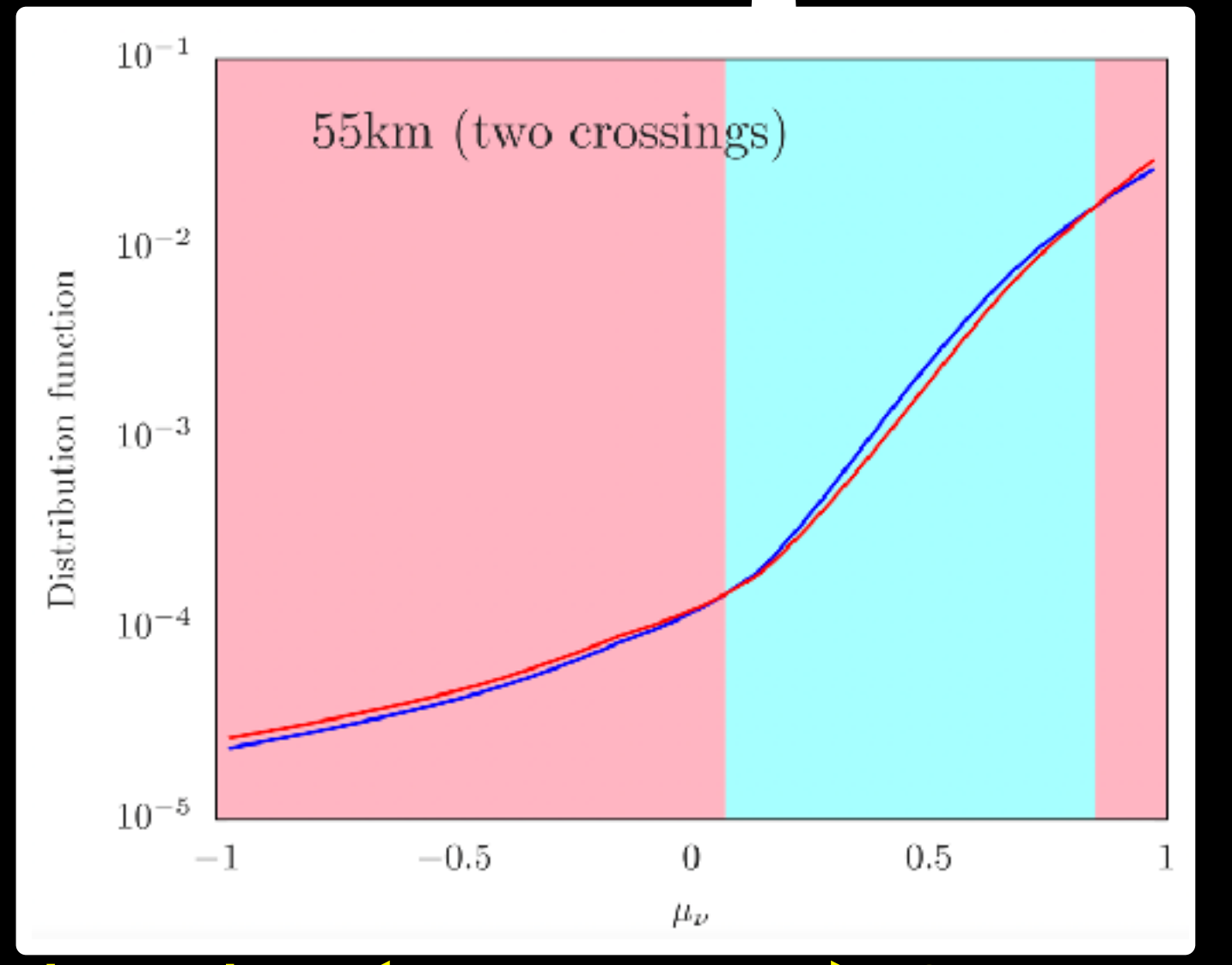
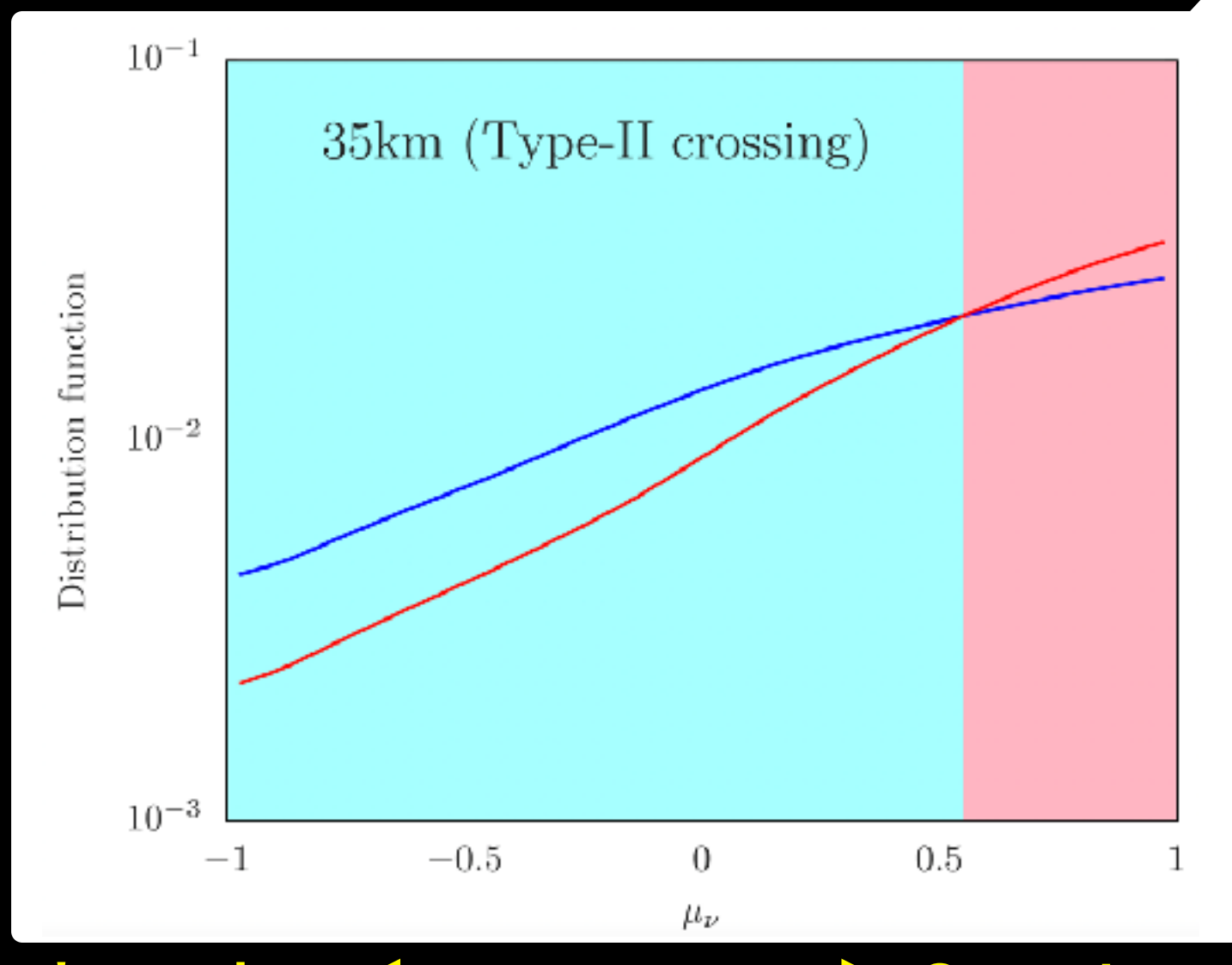
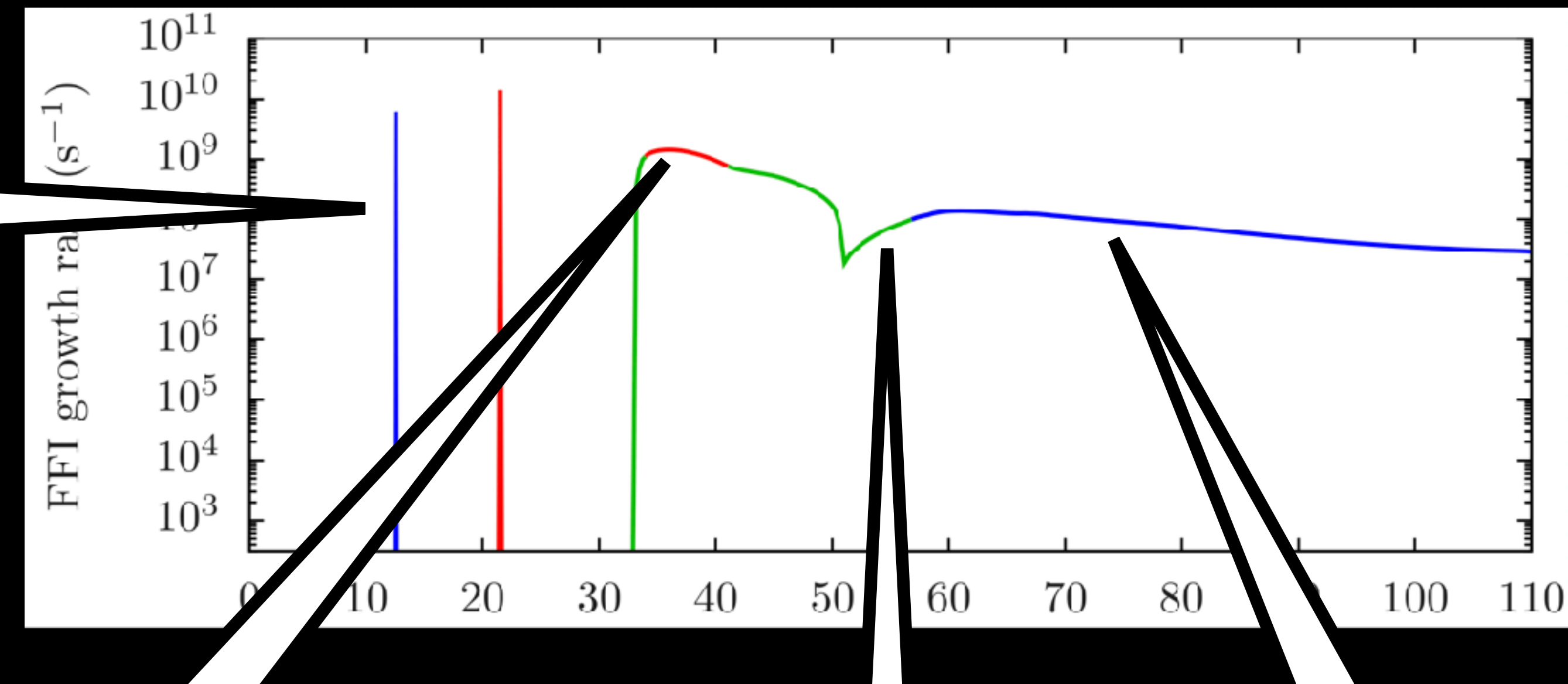


Properties of FFI

Neutrino chemical potential $\mu = 0$

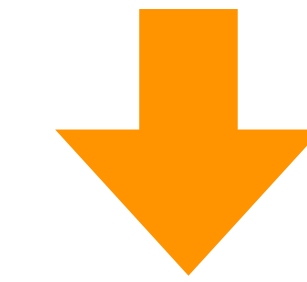


$$n_{\nu_e} \sim n_{\bar{\nu}_e}$$

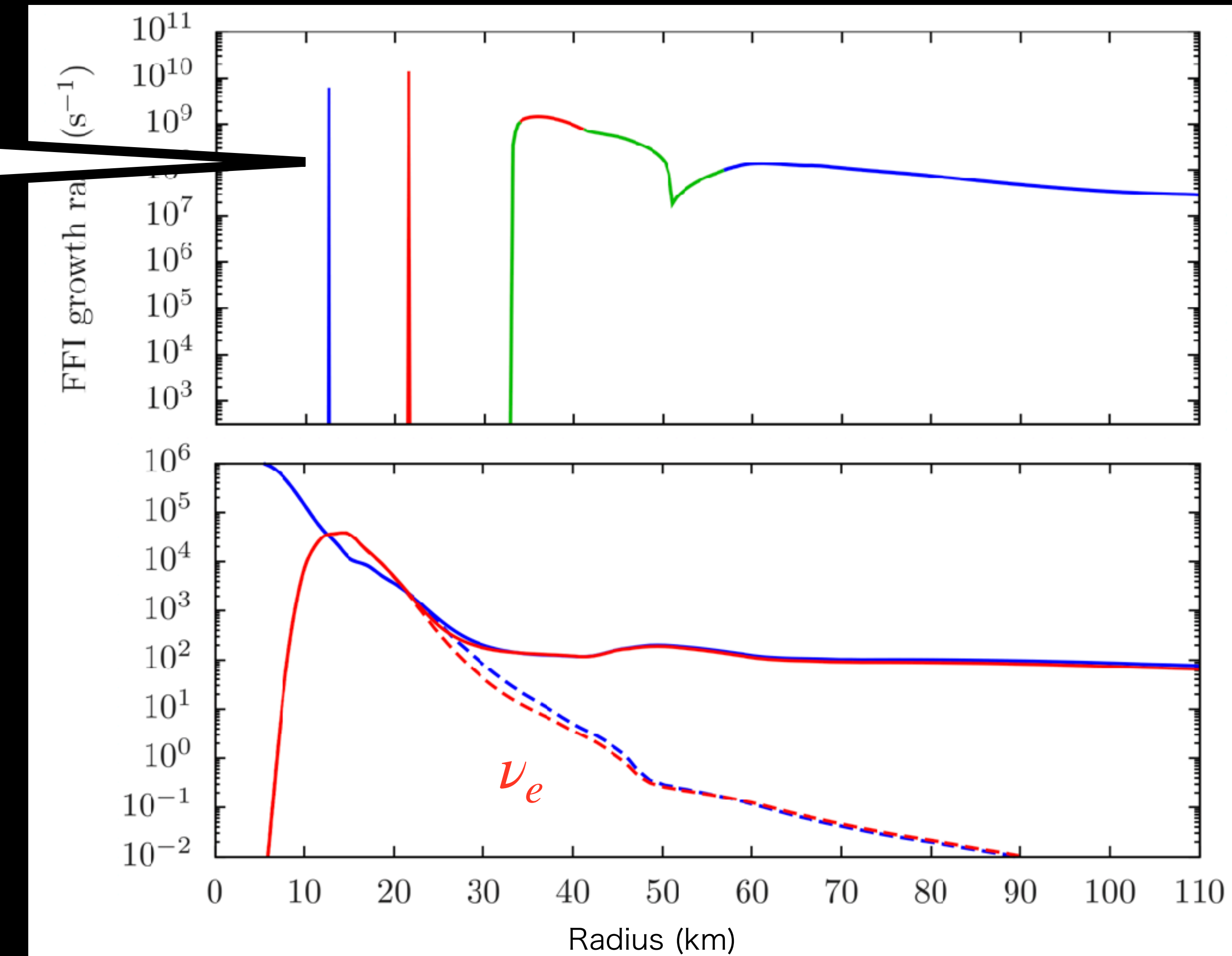


Properties of FFI

Neutrino chemical potential $\mu = 0$

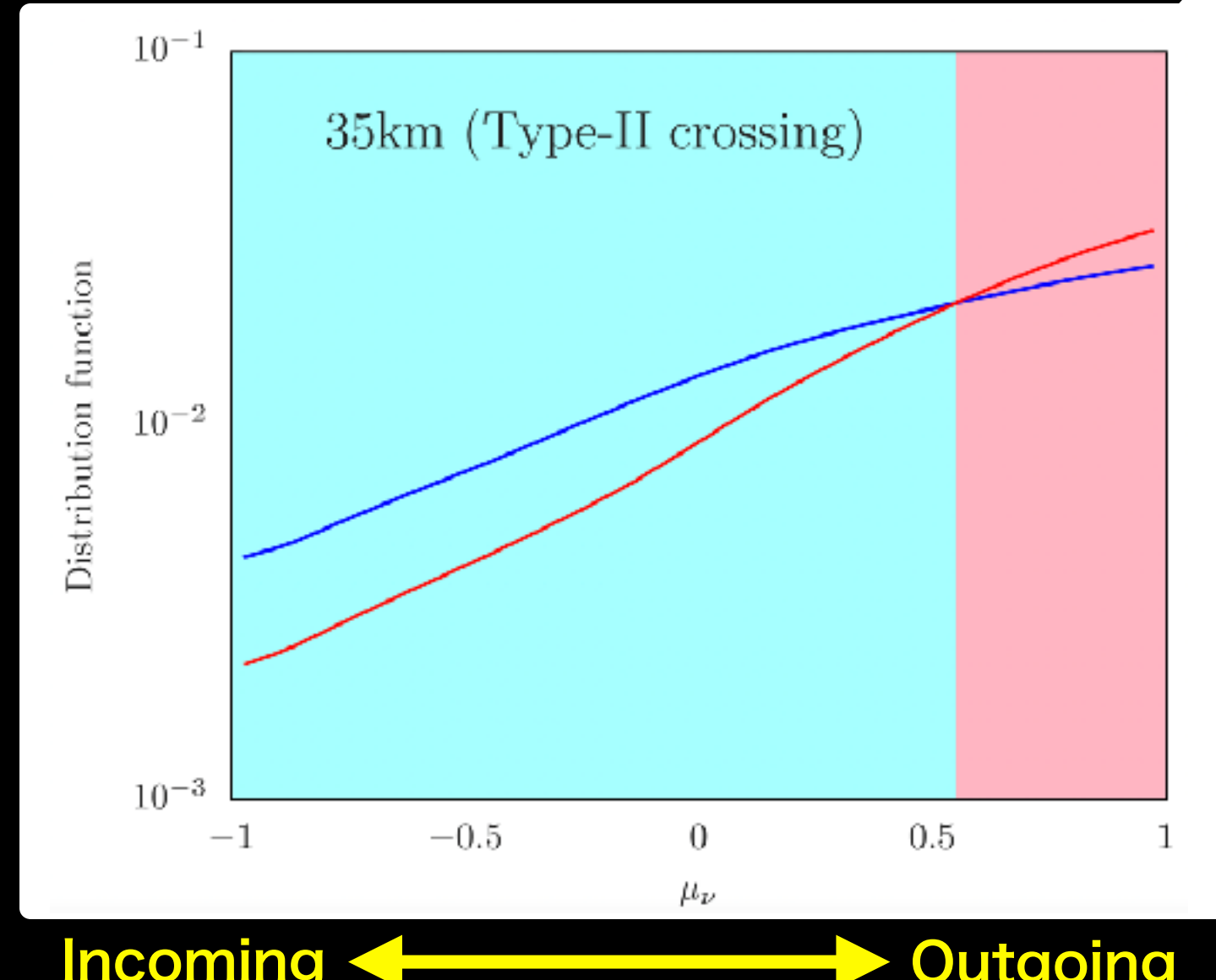


$$n_{\nu_e} \sim n_{\bar{\nu}_e}$$

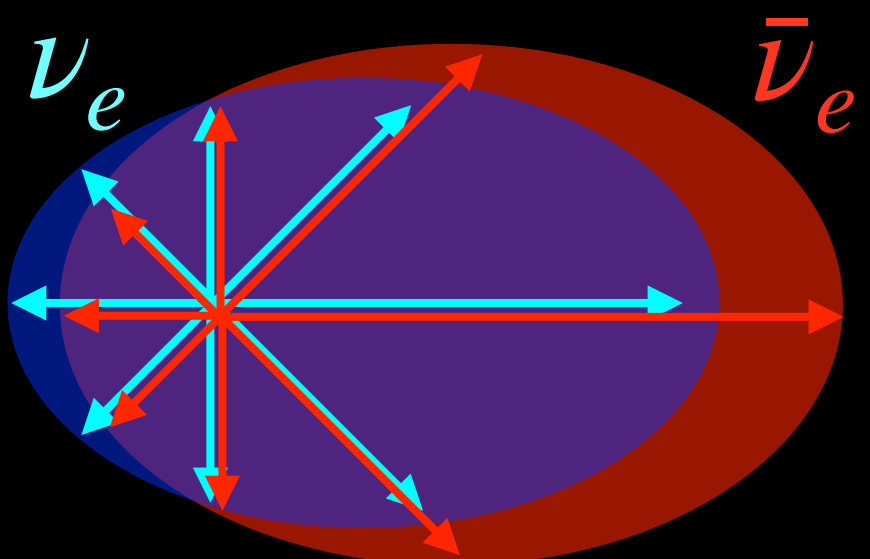


Properties of FFI

Angular distributions

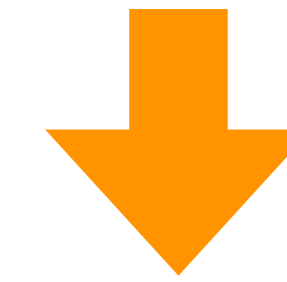


In between $\bar{\nu}_e$ sphere (inside) and ν_e sphere (outside), there is a region where $\bar{\nu}_e$ becomes more forward-peaked than ν_e

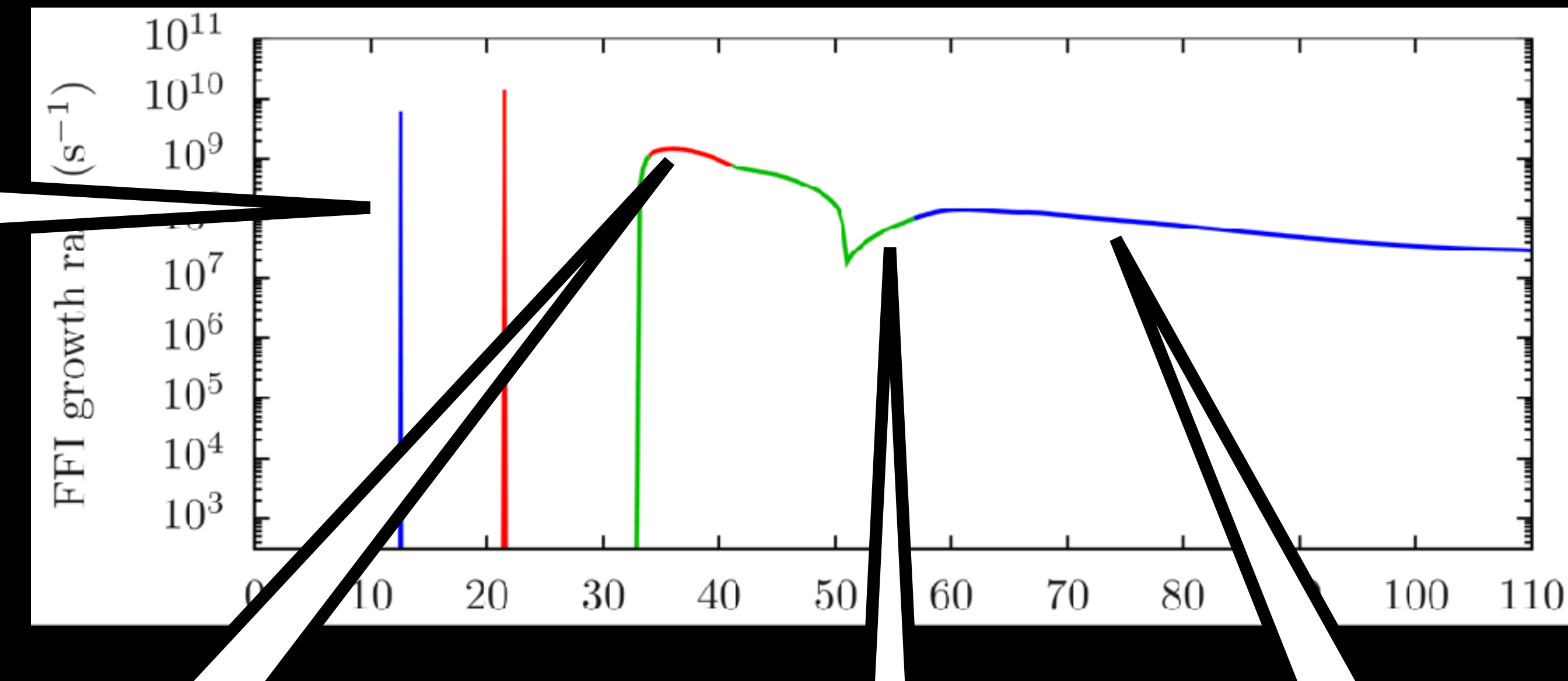


Properties of FFI

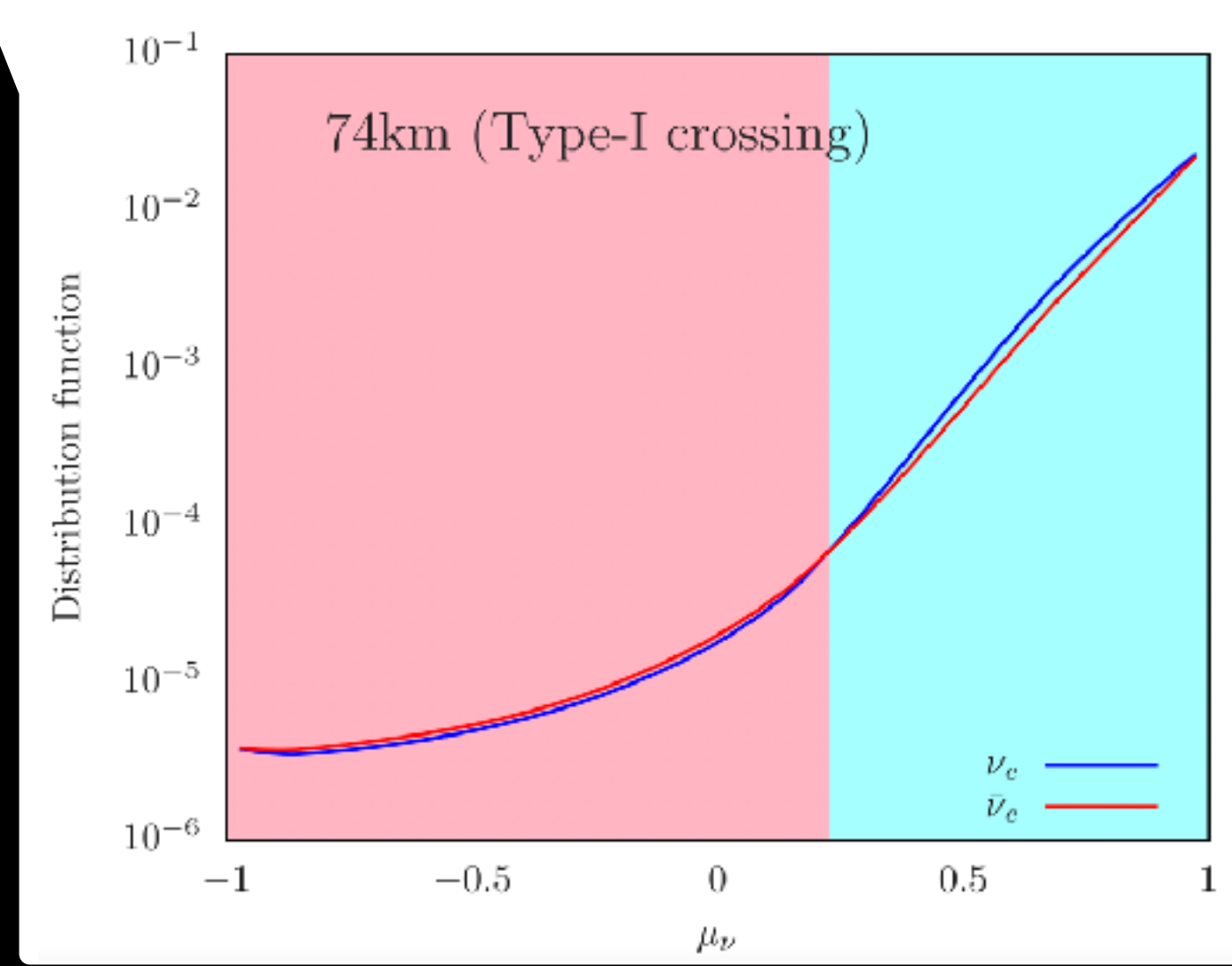
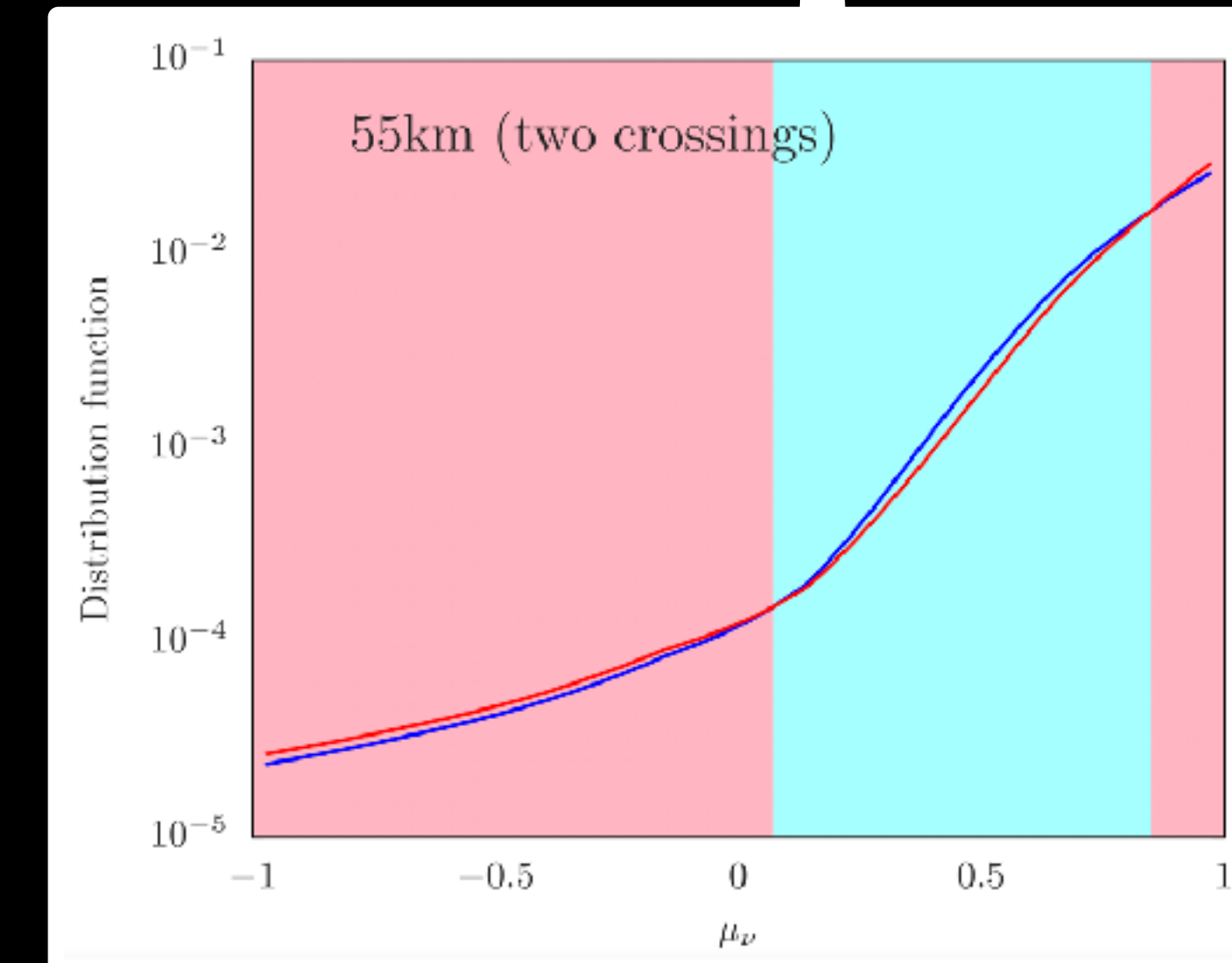
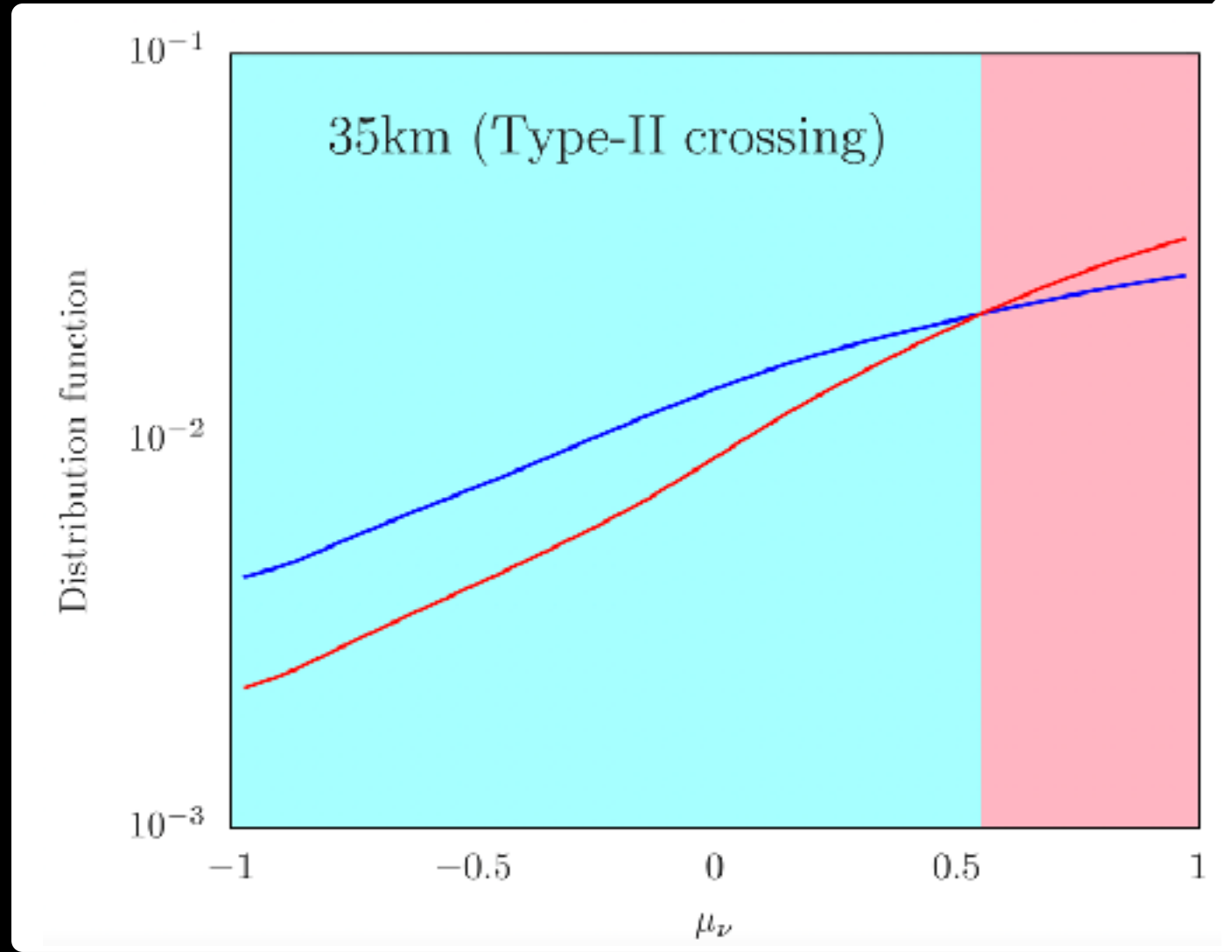
Neutrino chemical potential $\mu = 0$



$$n_{\nu_e} \sim n_{\bar{\nu}_e}$$



Angular distributions



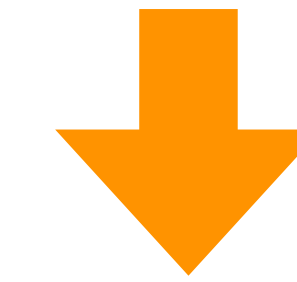
Incoming ← → Outgoing

Incoming ← → Outgoing

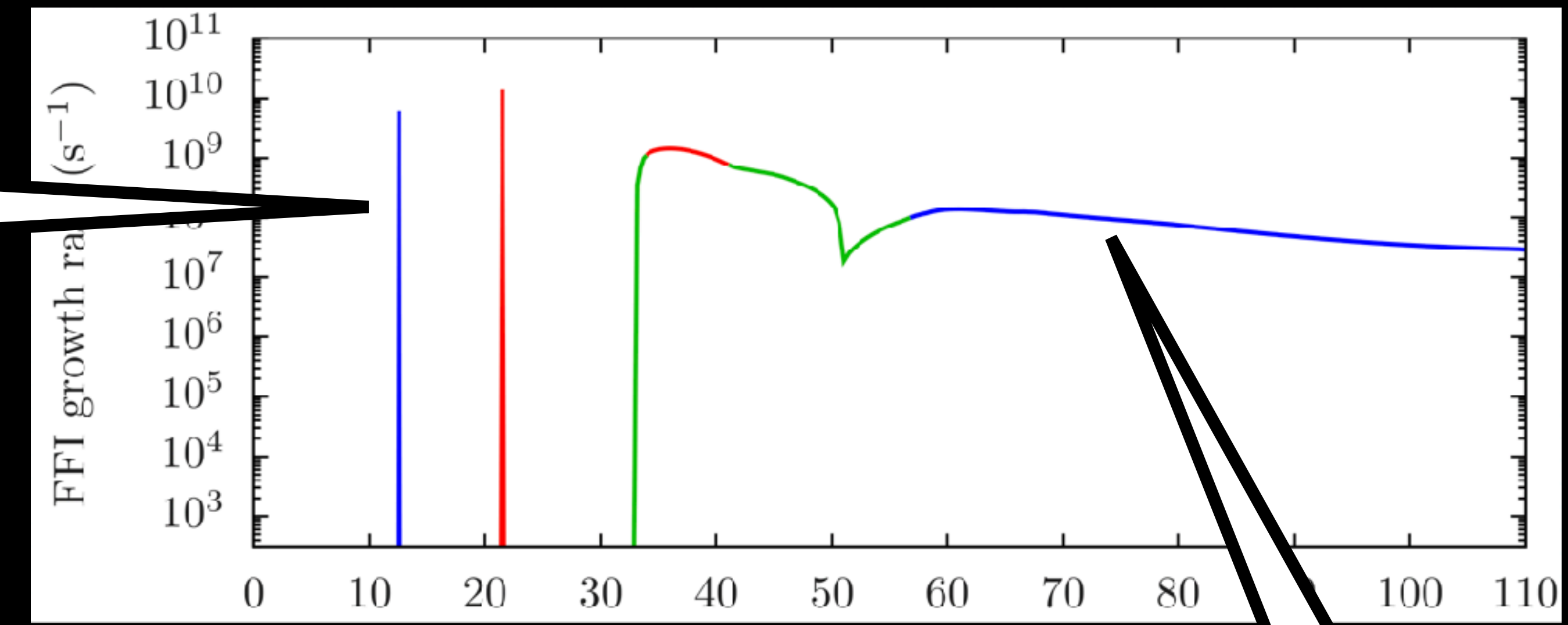
Incoming ← → Outgoing

Properties of FFI

Neutrino chemical potential $\mu = 0$

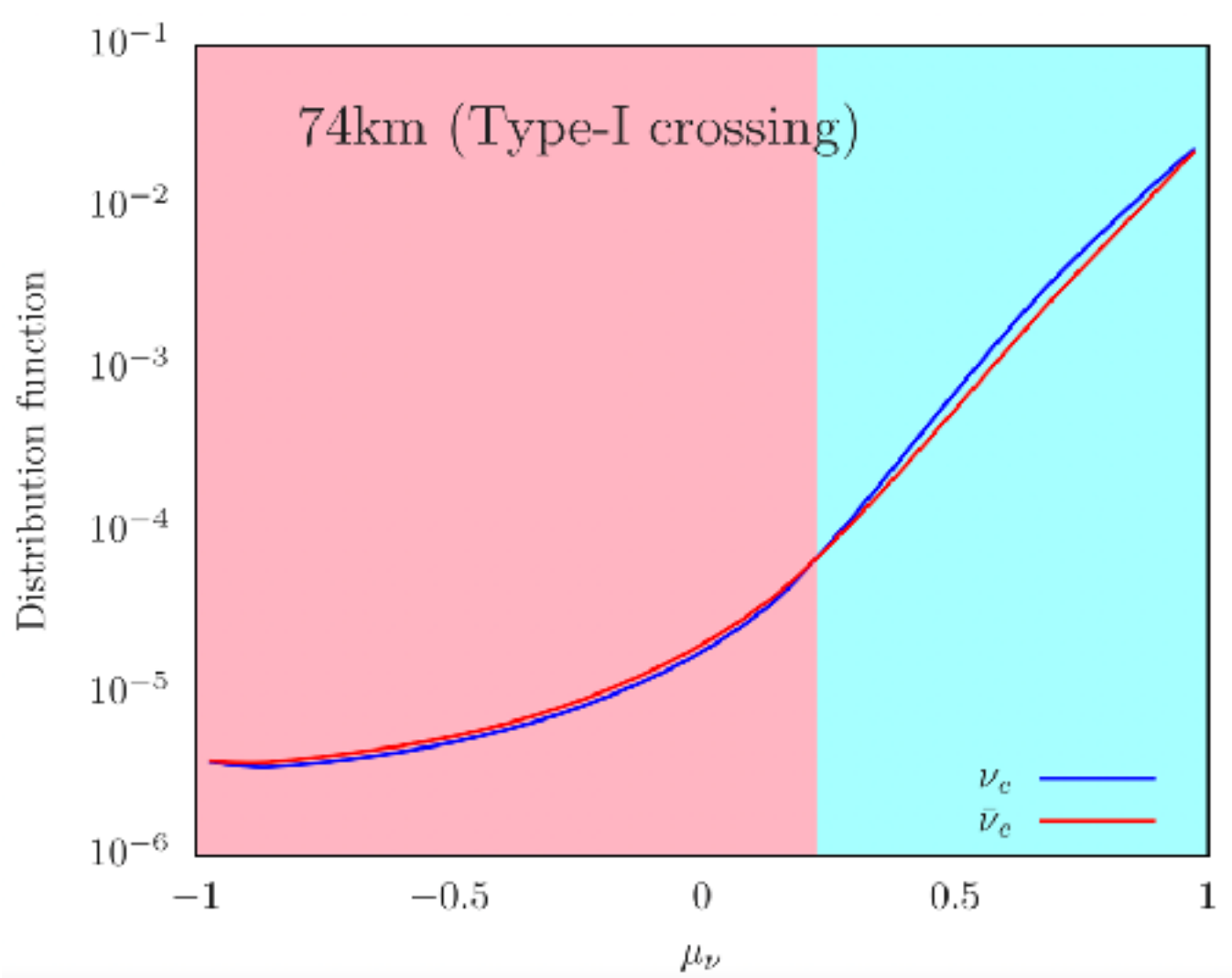
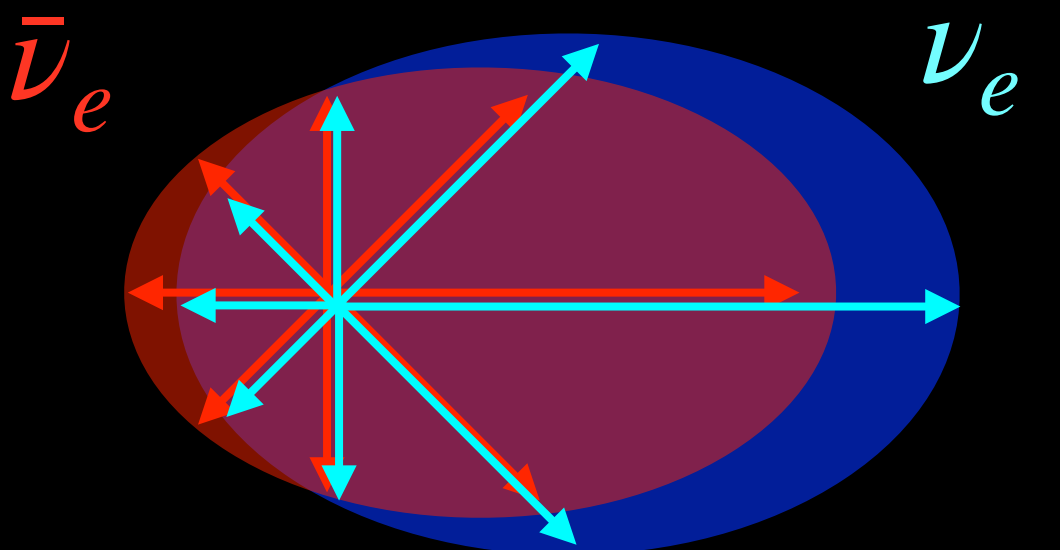


$$n_{\nu_e} \sim n_{\bar{\nu}_e}$$



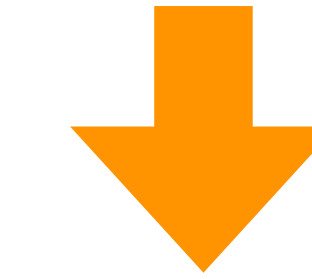
Angular distributions

Since $\bar{\nu}_e$ has higher mean energy, its back-scattering by nucleon dominates over ν_e

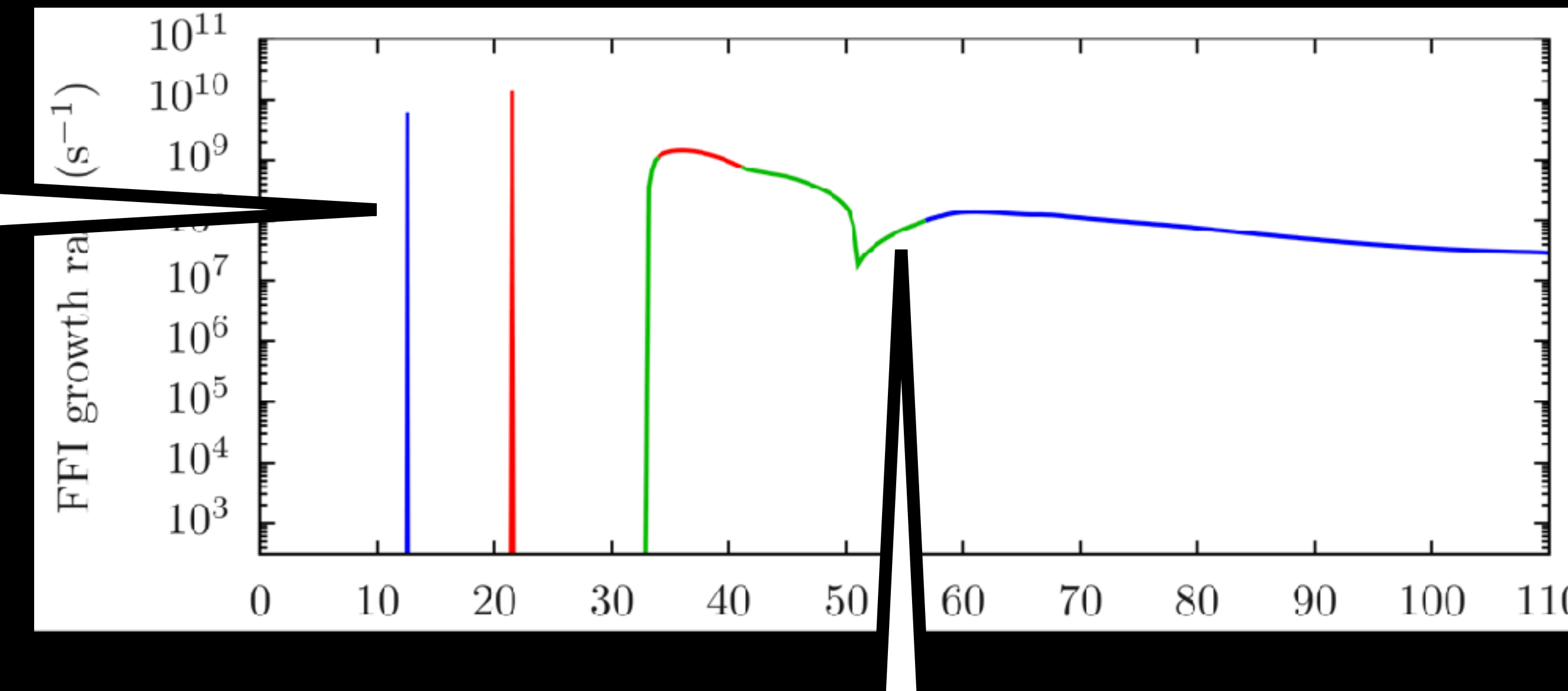


Properties of FFI

Neutrino chemical potential $\mu = 0$

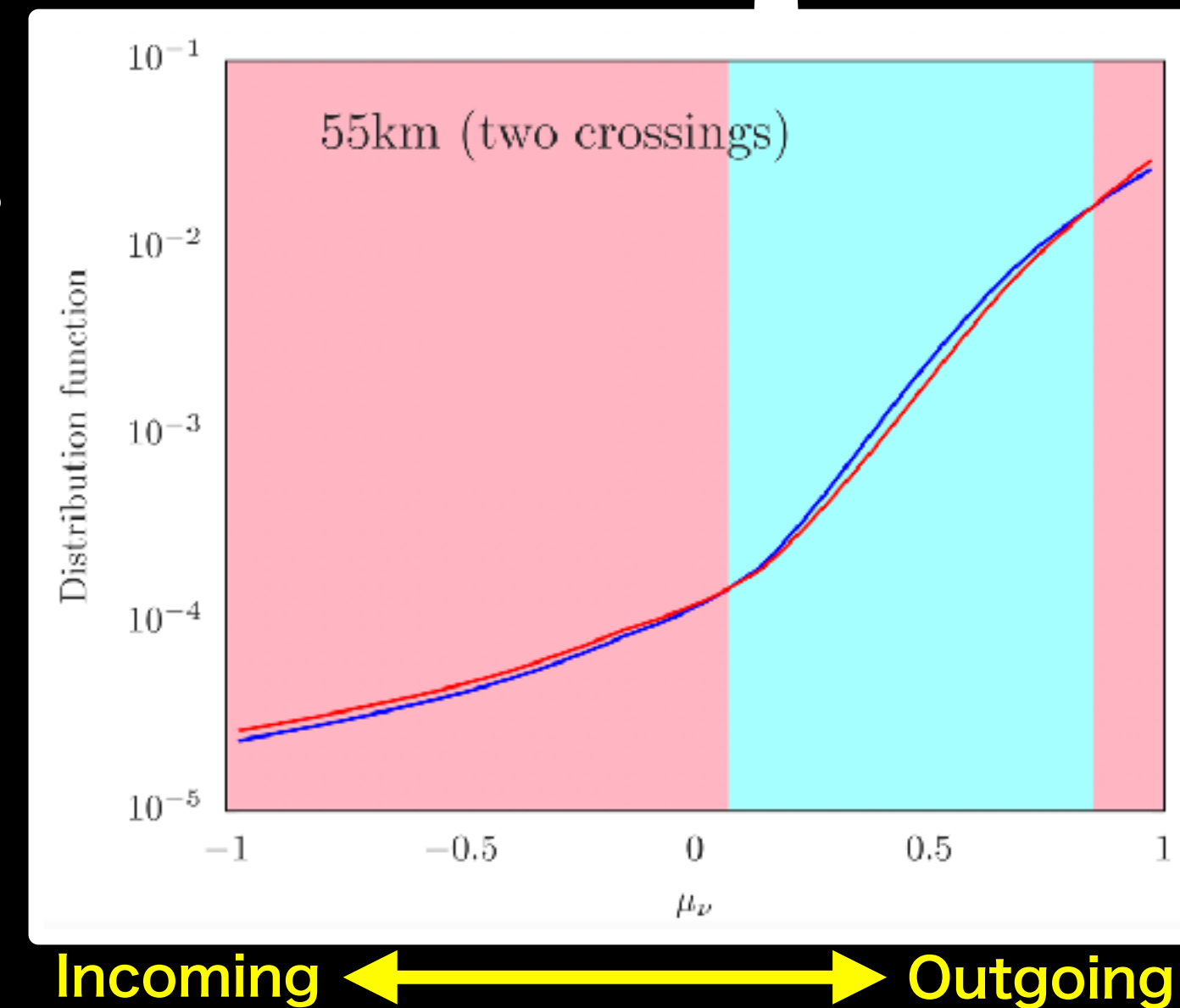
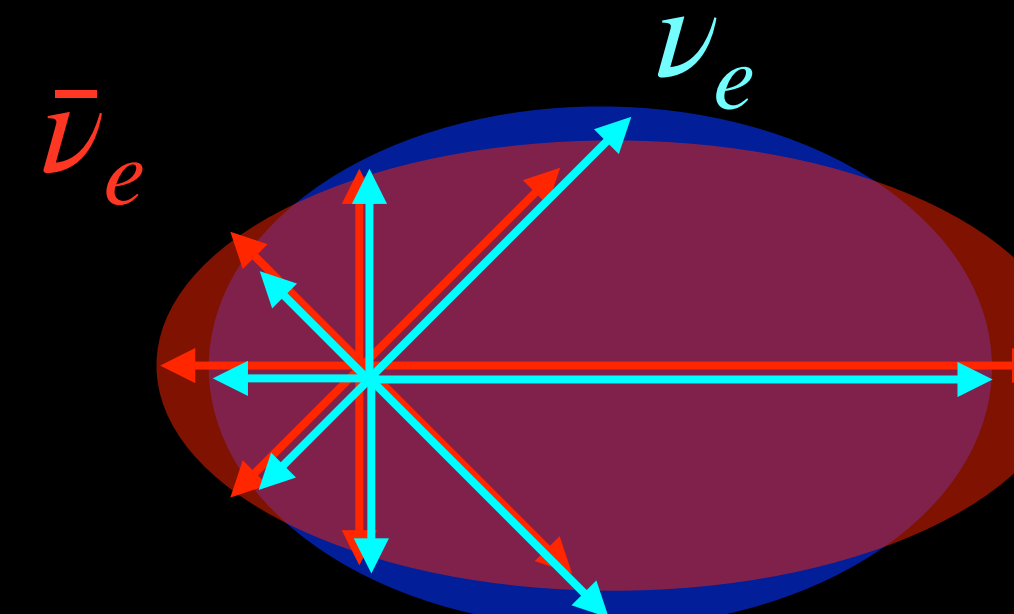


$$n_{\nu_e} \sim n_{\bar{\nu}_e}$$



Angular distributions

In the intermediate region, both mechanisms works and multiple crossing may appear

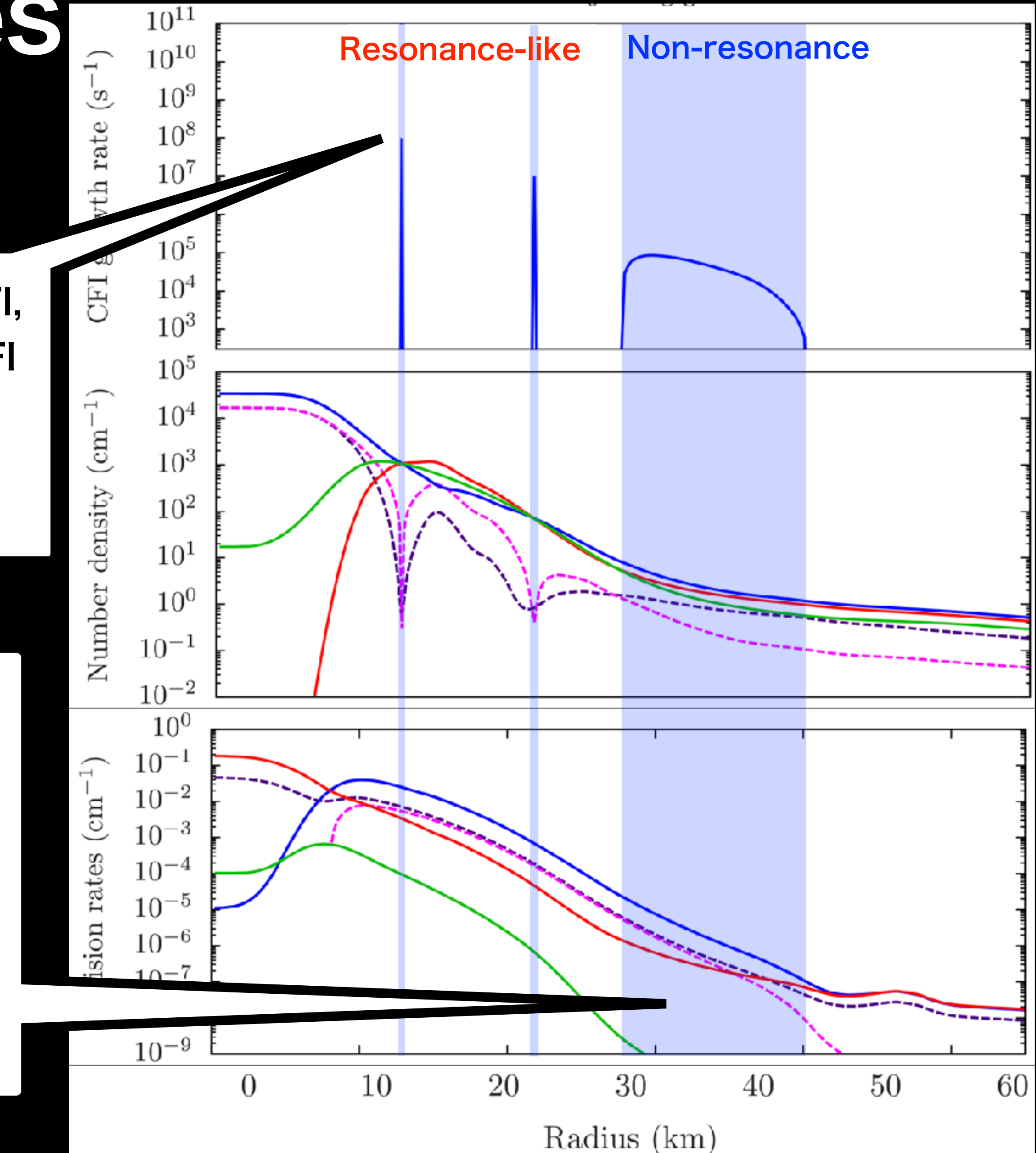


Properties of CFI

In the similar way as FFI,
 $\mu = 0$ is desirable for CFI

This region did not appear in previous 1D study (Liu, RA+ 2023)

- $n_{\nu_e} > n_{\nu_x}$ & $n_{\bar{\nu}_e} > n_{\nu_x}$
 because only ν_x is decoupled
- $\Gamma_e \sim \bar{\Gamma}_e$ due to low- Y_e environment



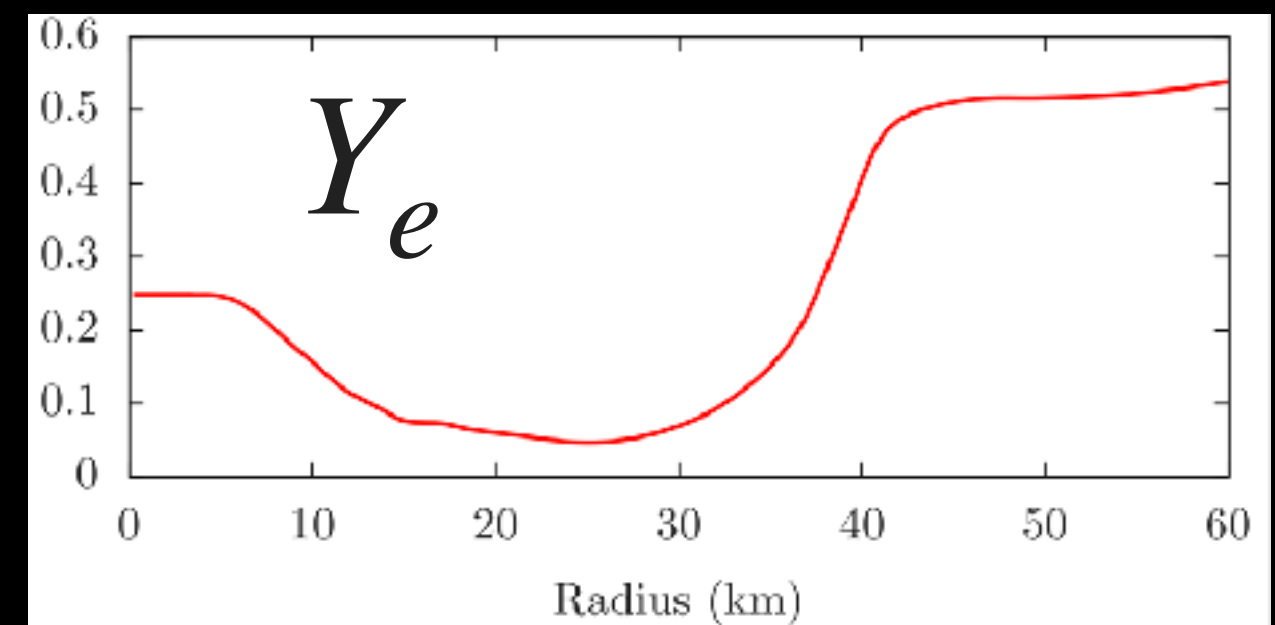
Non-resonance CFI (usual)

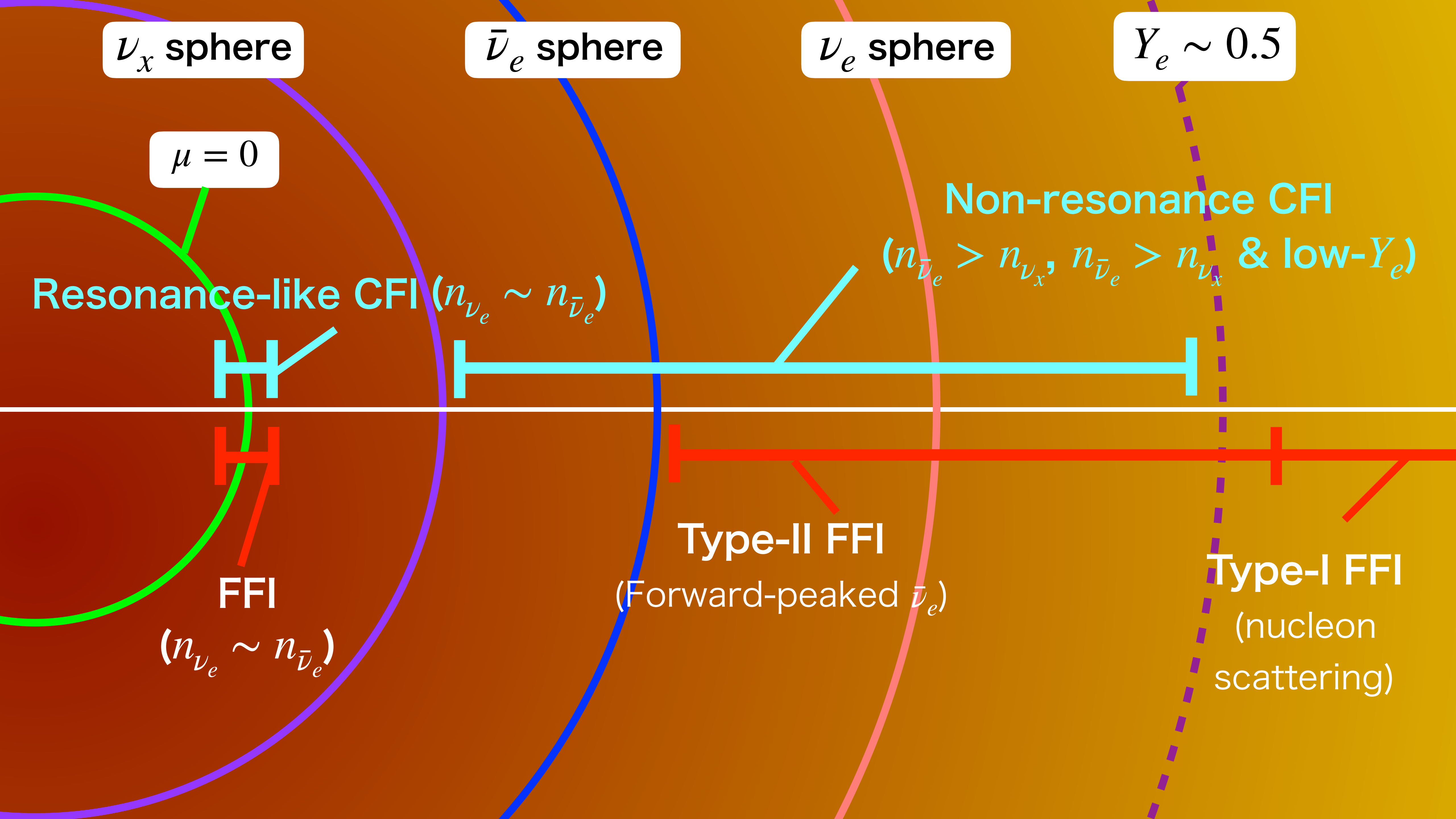
$$\sigma = \begin{cases} -\gamma + \frac{|G\alpha|}{|A|}, & (A^2 \gg |G\alpha|), \\ -\gamma + \sqrt{|G\alpha|}, & (A^2 \ll |G\alpha|) \end{cases}$$

Resonance-like CFI (Only when $A \sim 0$)

$$A = \frac{n_{\nu_e} - n_{\bar{\nu}_e}}{2} \quad G = \frac{n_{\nu_e} + n_{\bar{\nu}_e} - 2n_{\nu_x}}{2}$$

$$\gamma = \frac{\Gamma_e + \bar{\Gamma}_e + 2\Gamma_x}{2} \quad \alpha = \frac{\Gamma_e - \bar{\Gamma}_e}{2}$$

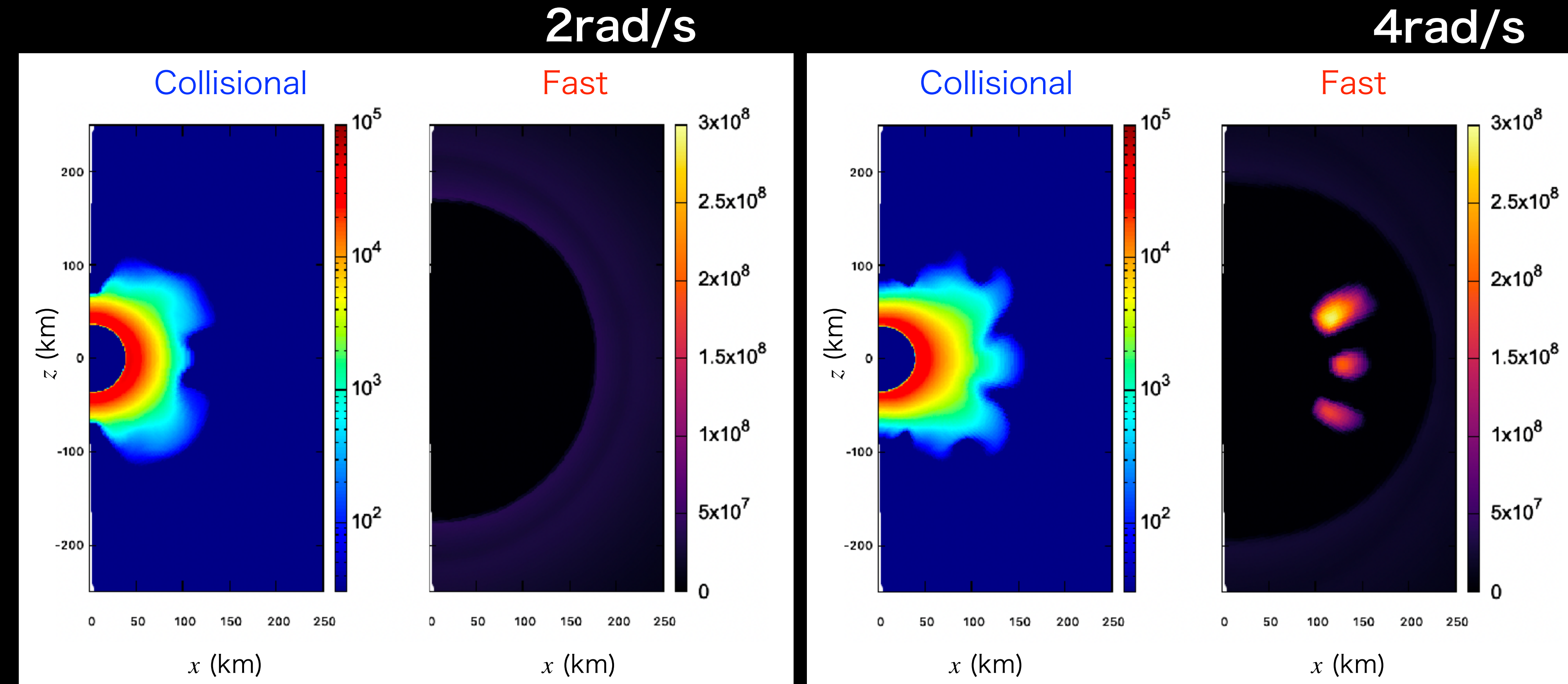




Effect of the Stellar Rotation

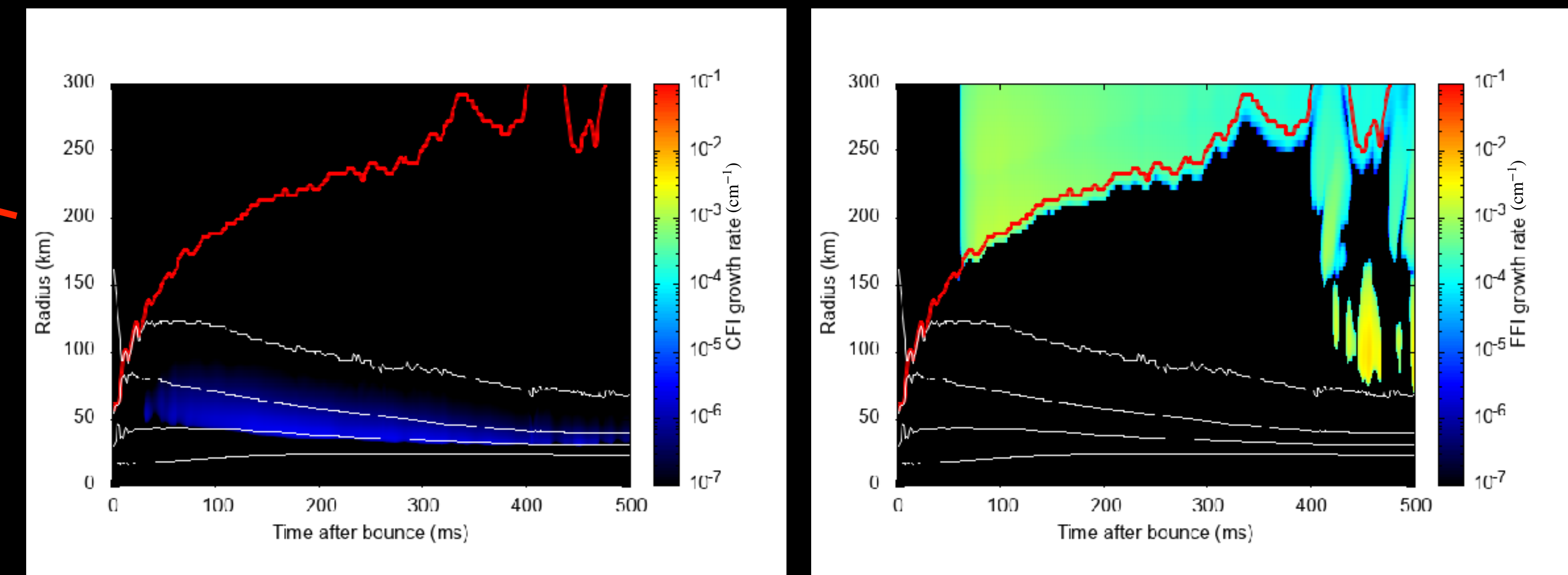
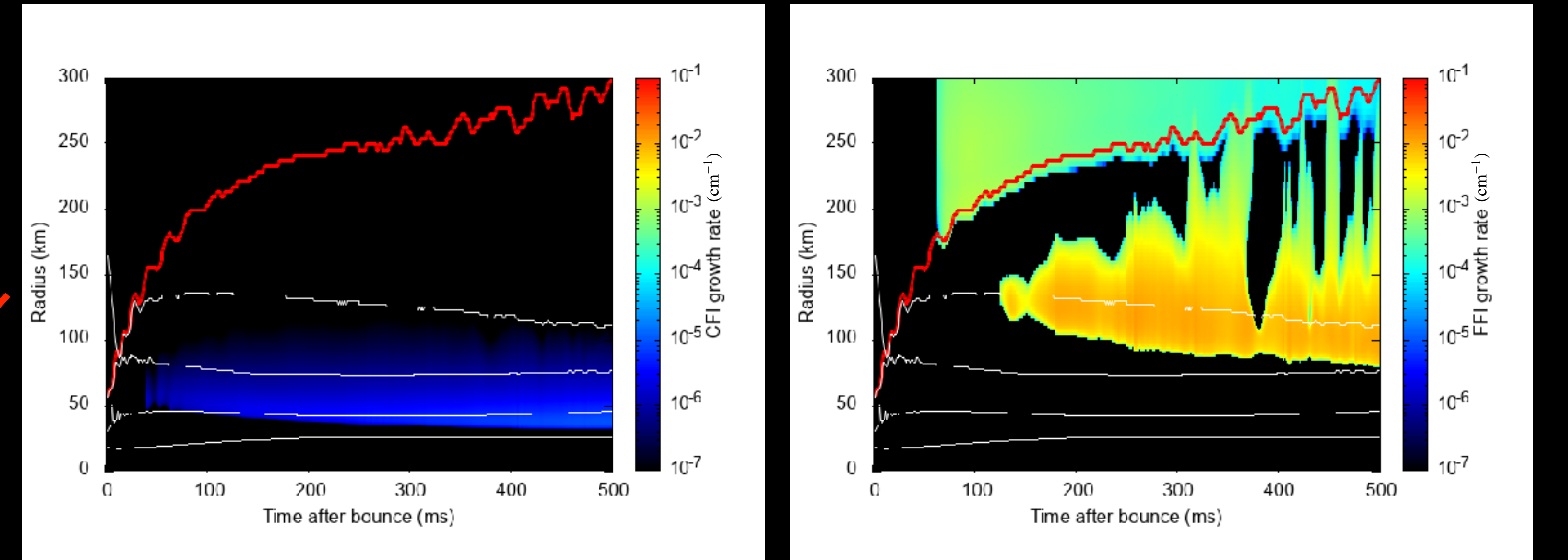
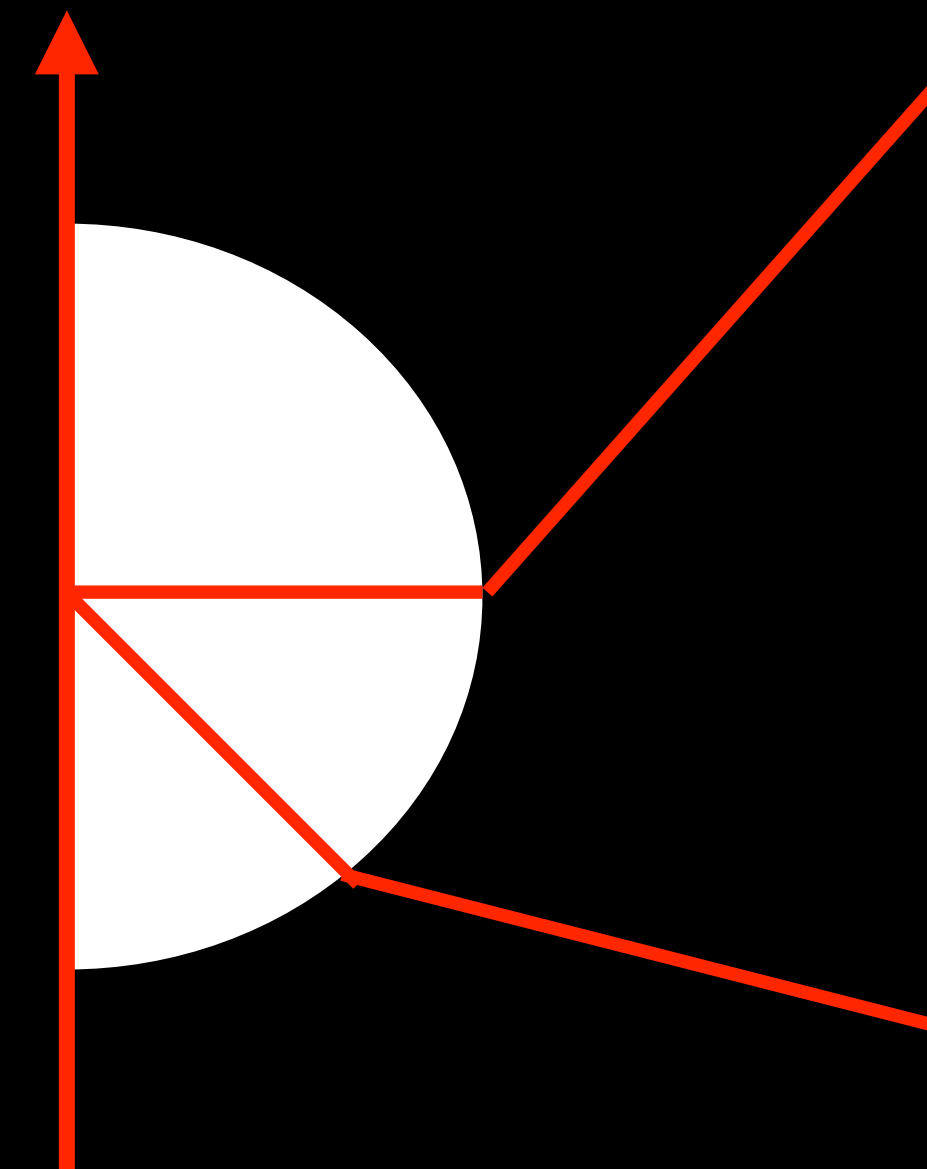
- Due to the centrifugal force, low- Y_e matter expands to the equatorial direction, which results in the enhancement of both FFI and CFI.

Furusawa-Togashi EOS
 $15M_{\odot}$ progenitor
Angular momentum distribution:
 $\frac{2, 4 \text{ rad/s}}{1 + (r/10^3 \text{ km})^2}$



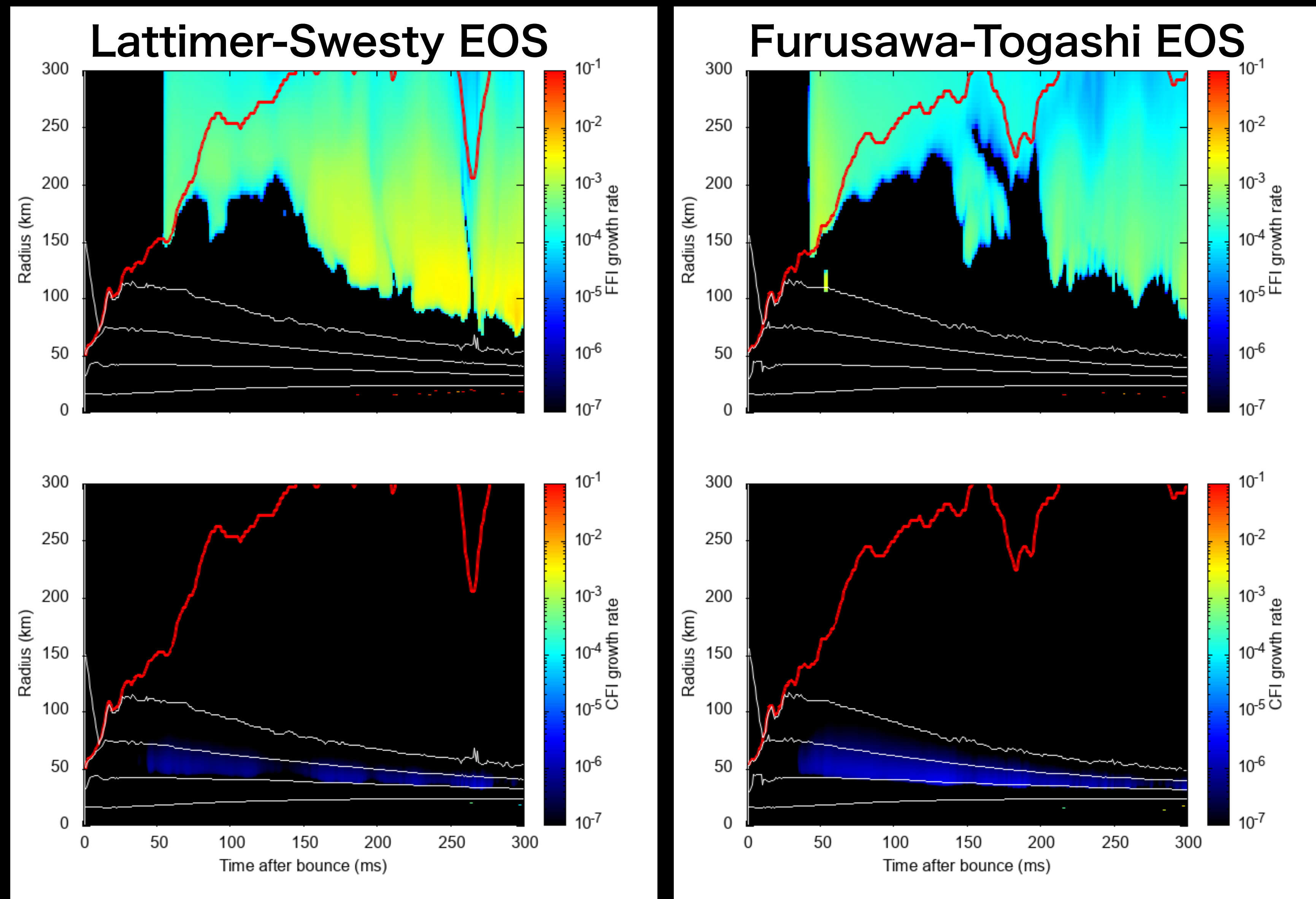
Effect of the Stellar Rotation

Rotation axis



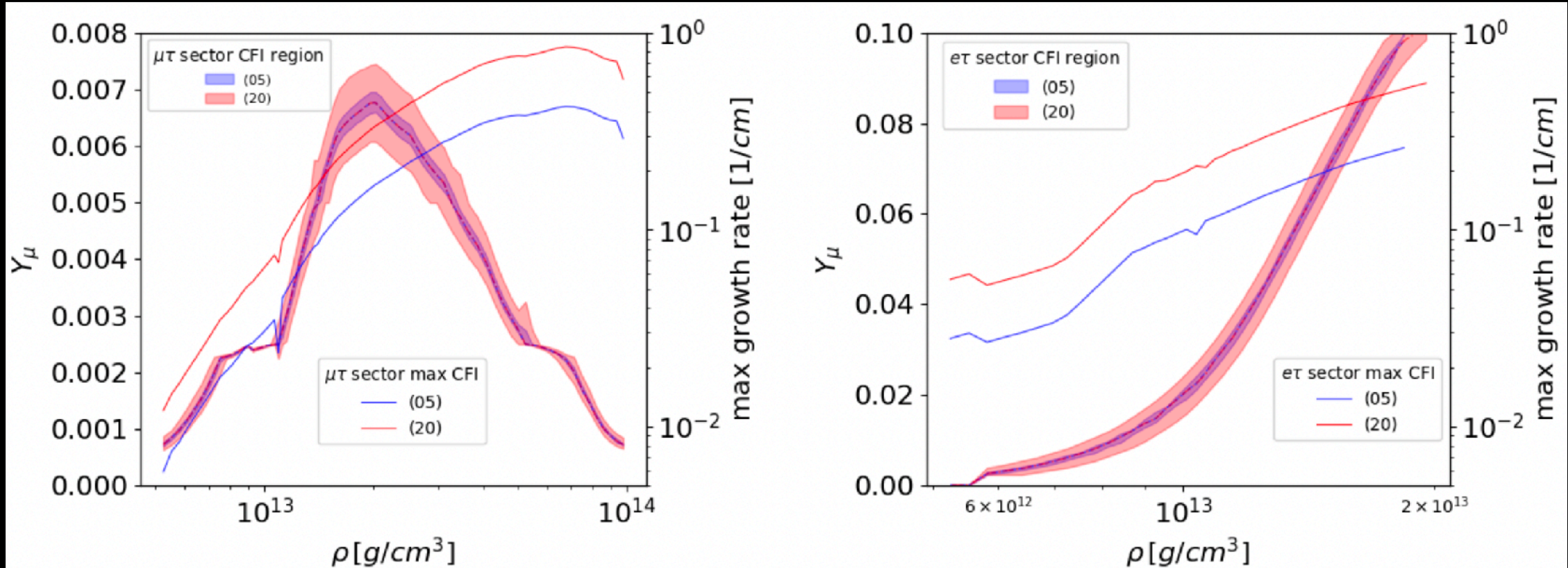
EOS Dependence

$11.2M_{\odot}$ progenitor



Effects of Muon on CFI (arXiv:2407.10604)

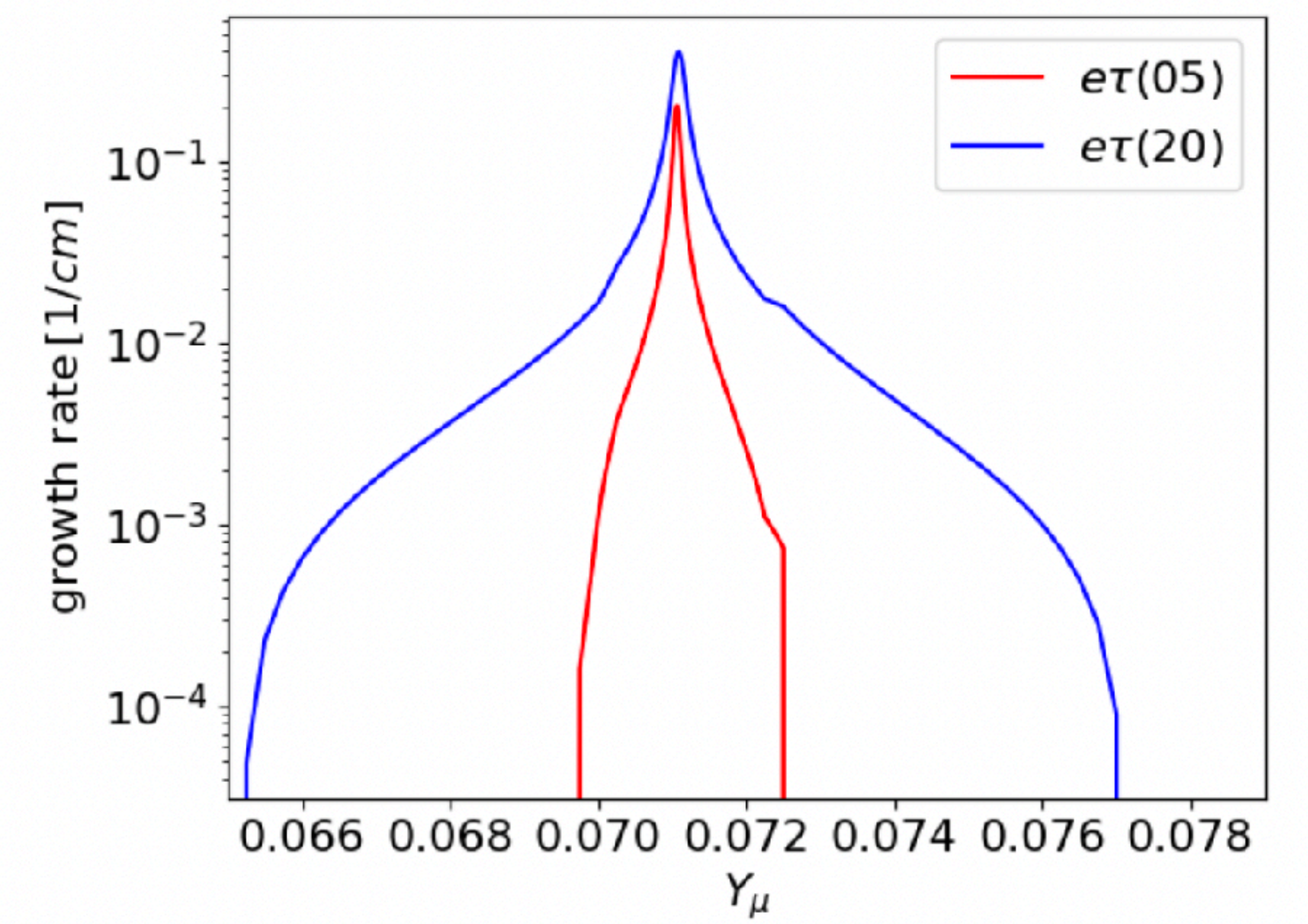
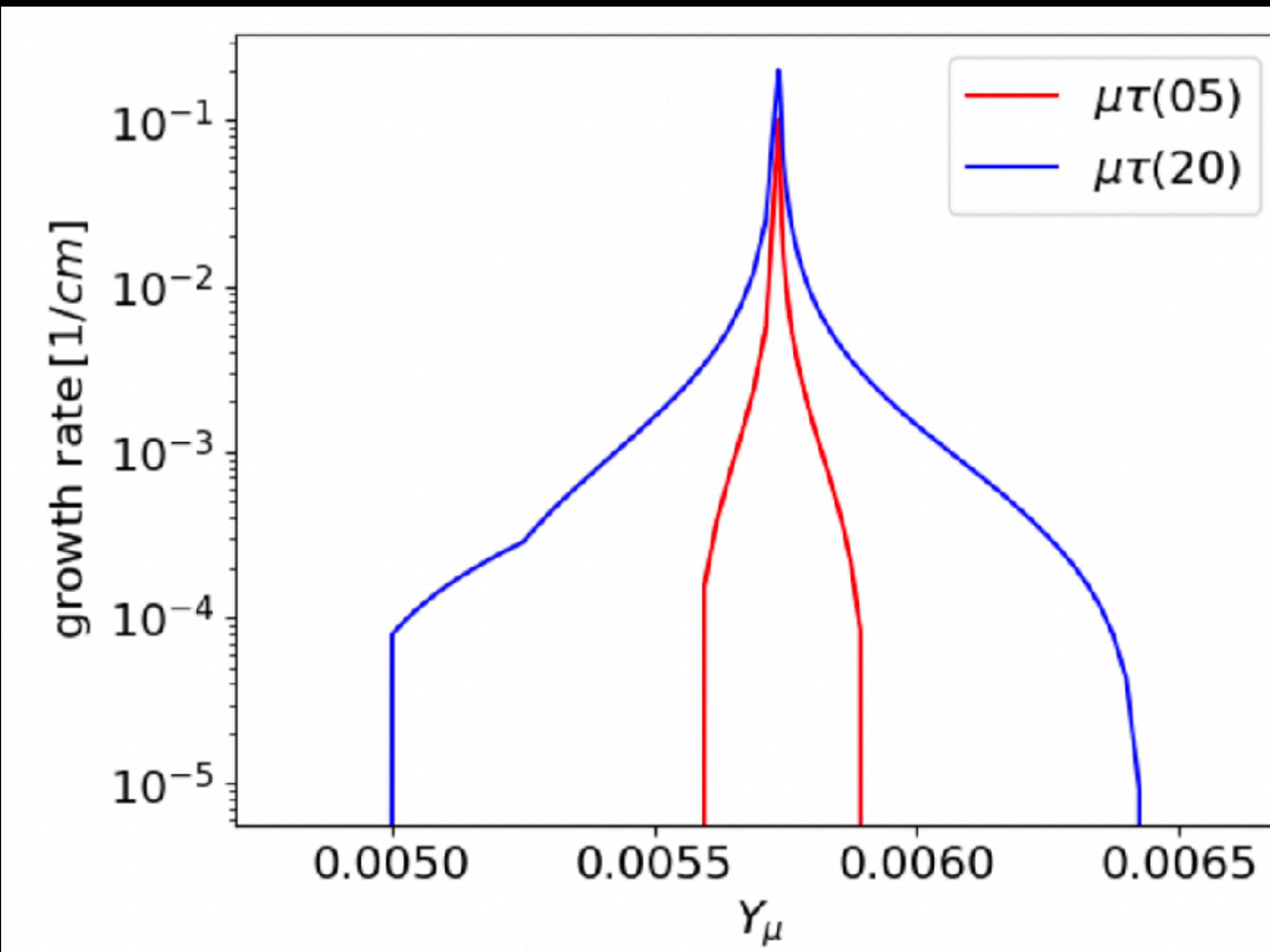
In CCSNe, muons can also appear in CCSNe (Boling 2017)



$$\sigma = \begin{cases} -\gamma + \frac{|G\alpha|}{|A|}, & (A^2 \gg |G\alpha|), \\ -\gamma + \sqrt{|G\alpha|}, & (A^2 \ll |G\alpha|) \end{cases}$$

$$G \equiv \frac{n_{\nu_i} + n_{\bar{\nu}_i} - n_{\nu_j} - n_{\bar{\nu}_j}}{2} \quad \alpha \equiv \frac{\Gamma_{\nu_i} - \Gamma_{\bar{\nu}_i} + \Gamma_{\nu_j} - \Gamma_{\bar{\nu}_j}}{2}$$
$$A \equiv \frac{n_{\nu_i} - n_{\bar{\nu}_i} - n_{\nu_j} + n_{\bar{\nu}_j}}{2} \quad \gamma \equiv \frac{\Gamma_{\nu_i} + \Gamma_{\bar{\nu}_i} + \Gamma_{\nu_j} + \Gamma_{\bar{\nu}_j}}{2}$$

Effects of Muon on CFI



Discussion

- FFI & CFI commonly occurs in CCSNe
- FFI growth rate is orders of magnitude larger than CFI if they occur in the same place. However, CFI occurs at inner radii (upstream), which may modify the appearance of FFI at larger radii.

Future Tasks

- Classical simulation + back-reaction of flavor conversion (such as Ehring+2023)